Simulating the Universe with SPH – A mixed blessing

Volker Springel

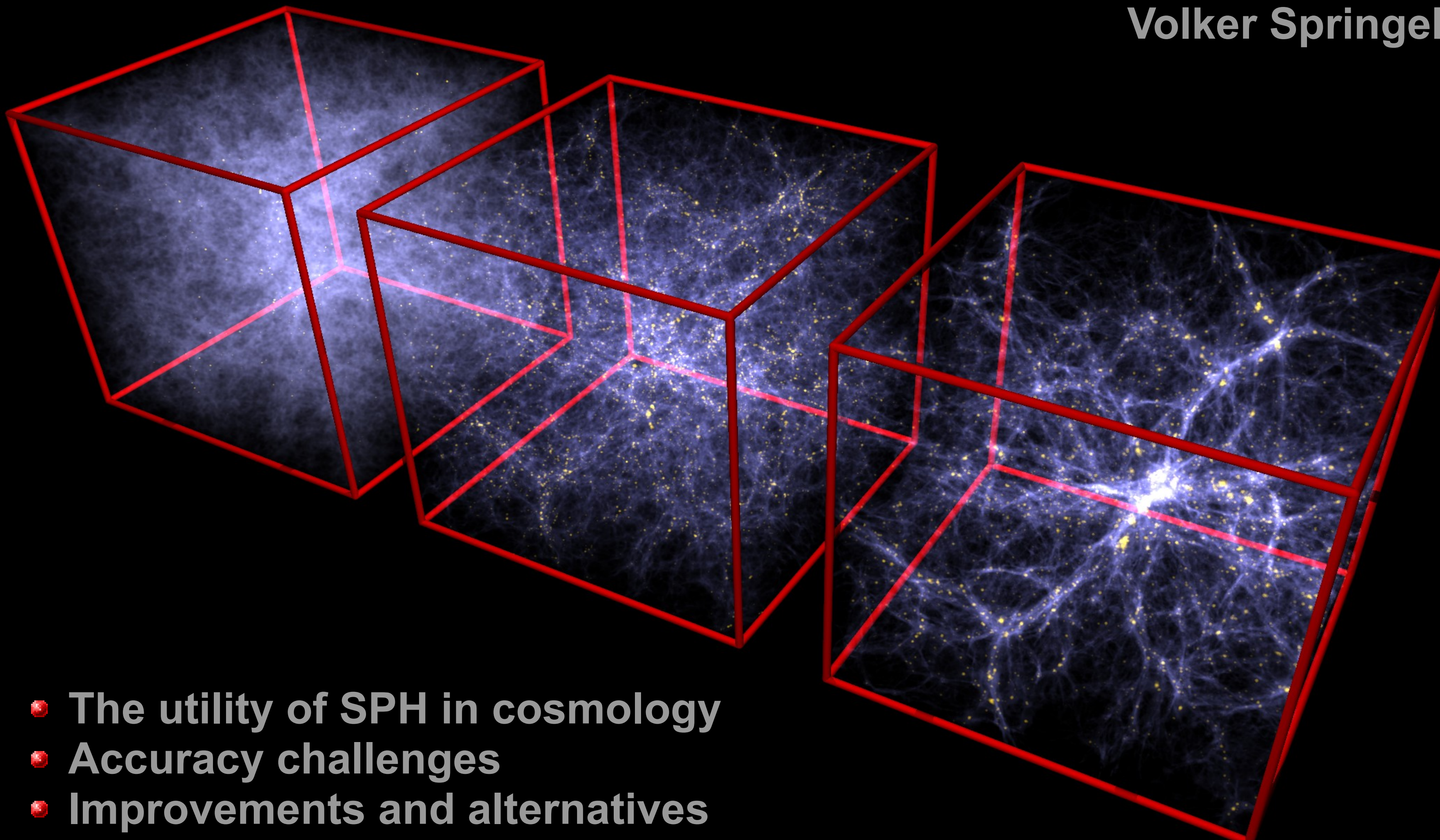

- The utility of SPH in cosmology
- Accuracy challenges
- Improvements and alternatives

Heidelberg Institute for Theoretical Studies

HITS

Universität Heidelberg

6th SPHERIC Workshop
Hamburg, June 2011

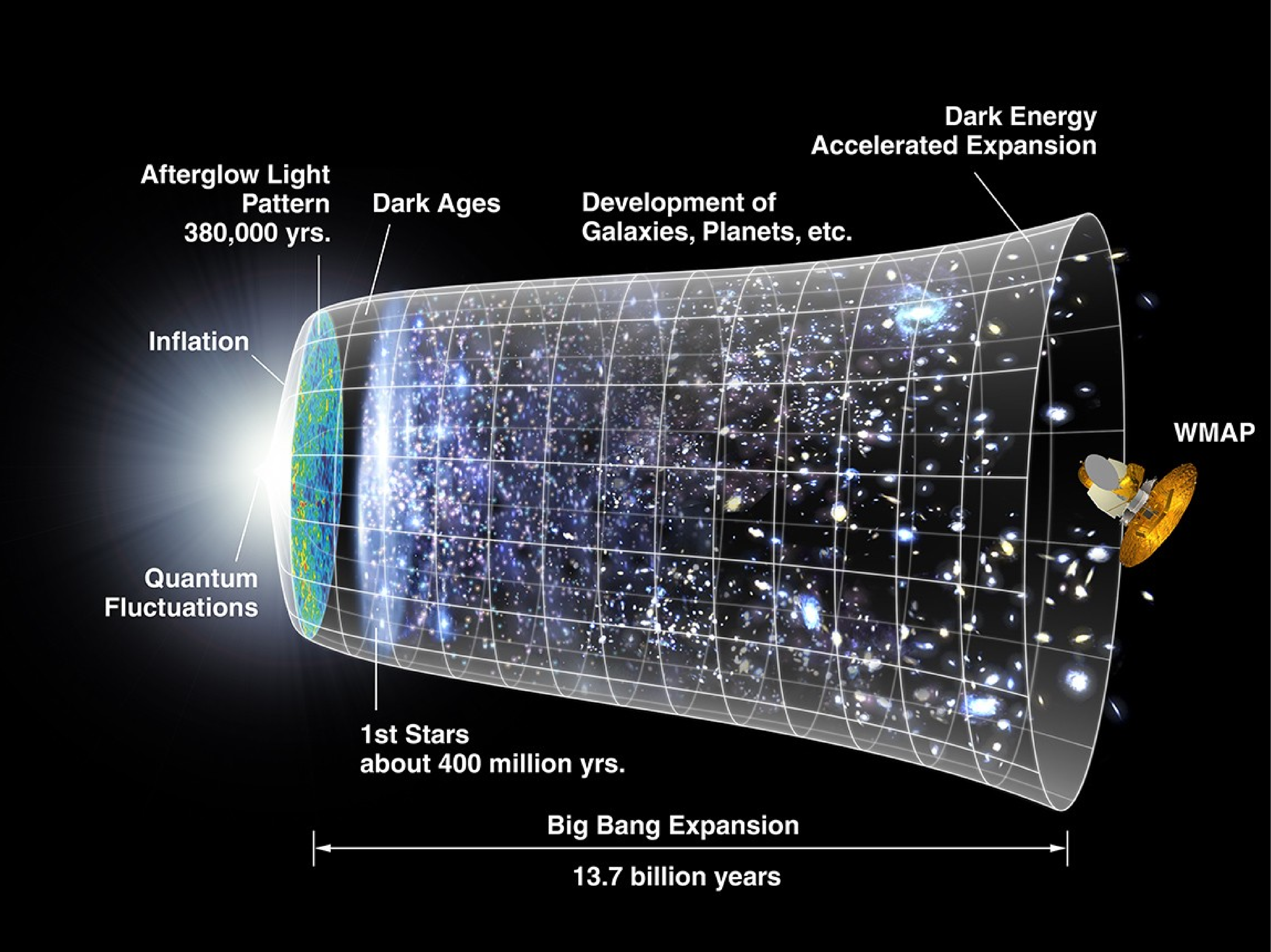
Dark Energy
Accelerated Expansion
Afterglow Light
Pattern
380,000 yrs.
Dark Ages
Development of
Galaxies, Planets, etc.
Inflation
WMAP
Quantum
Fluctuations
1st Stars
about 400 million yrs.
Big Bang Expansion
13.7 billion years

The basic dynamics of structure formation in baryonic matter

BASIC EQUATIONS

Astrophysical plasmas are extremely thin, with (usually) negligible viscosity

Euler equations of inviscid ideal gas dynamics

$$\frac{\partial \rho_c}{\partial t} + \frac{1}{a}\boldsymbol{\nabla}_c(\rho_c \boldsymbol{v}) = 0$$

$$\frac{\partial(\rho_c \boldsymbol{v})}{\partial t} + \frac{1}{a}\boldsymbol{\nabla}_c[(\rho_c \boldsymbol{v}\boldsymbol{v}^T + P_c)\boldsymbol{v}] = -H(a)\,\rho_c \boldsymbol{v} - \frac{\rho_c}{a^2}\boldsymbol{\nabla}_c \Phi_c$$

$$\frac{\partial(\rho_c e)}{\partial t} + \frac{1}{a}\boldsymbol{\nabla}_c[(\rho_c e + P_c)\boldsymbol{v}] = -2H(a)\,\rho_c e - \frac{\rho_c \boldsymbol{v}}{a^2}\boldsymbol{\nabla}_c \Phi_c$$

$$\nabla_c^2 \Phi_c = 4\pi G\,[\rho_c(\boldsymbol{x}) - \overline{\rho_c}]$$

Important hydrodynamical processes

Shock waves
Turbulence
Radiative transfer
Magnetic fields
Star formation
Supernova explosions
Black holes, etc...

For an adiabatic flow in SPH, temperature can be derived from the specific entropy

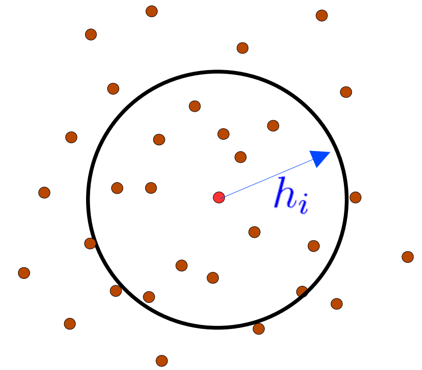

ENTROPY FORMALISM

Density estimate:

$$\rho_i = \sum_{j=1}^{N} m_j W(|\mathbf{r}_{ij}|, h_i)$$

Definition of an **entropic function**:

$$P_i = A_i \, \rho_i^{\gamma}$$

for an adiabatic flow:

$$A_i = A_i(s_i) = \text{const.}$$

Do not need to integrate the temperature, but can infer it from:

$$u_i = \frac{A_i}{\gamma - 1} \rho^{\gamma - 1}$$

Use an artificial viscosity to generate entropy in shocks:

$$\frac{\mathrm{d}A_i}{\mathrm{d}t} = \frac{1}{2} \frac{\gamma - 1}{\rho_i^{\gamma-1}} \sum_{j=1}^{N} m_j \Pi_{ij} \mathbf{v}_{ij} \cdot \nabla_i \overline{W}_{ij}$$

A fully conservative formulation of SPH

Springel & Hernquist (2002)
Monaghan (2002)

DERIVATION

Lagrangian:

$$L(\mathbf{q}, \dot{\mathbf{q}}) = \frac{1}{2}\sum_{i=1}^{N} m_i \dot{\mathbf{r}}_i^2 - \frac{1}{\gamma - 1}\sum_{i=1}^{N} m_i A_i \rho_i^{\gamma-1}$$

$$\mathbf{q} = (\mathbf{r}_1, \ldots, \mathbf{r}_N, h_1, \ldots, h_N)$$

Constraints:

$$\phi_i(\mathbf{q}) \equiv \frac{4\pi}{3} h_i^3 \rho_i - M_{\rm sph} = 0$$

Equations of motion:

$$\frac{\mathrm{d}}{\mathrm{d}t}\frac{\partial L}{\partial \dot{q}_i} - \frac{\partial L}{\partial q_i} = \sum_{j=1}^{N} \lambda_j \frac{\partial \phi_j}{\partial q_i}$$

$$\frac{\mathrm{d}\mathbf{v}_i}{\mathrm{d}t} = -\sum_{j=1}^{N} m_j \left[f_i \frac{P_i}{\rho_i^2} \nabla_i W_{ij}(h_i) + f_j \frac{P_j}{\rho_j^2} \nabla_i W_{ij}(h_j) \right]$$

$$f_i = \left[1 + \frac{h_i}{3\rho_i}\frac{\partial \rho_i}{\partial h_i} \right]^{-1}$$

SPH can handle strong shocks and vorticity generation

A MACH NUMBER 10 SHOCK THAT STRIKES AN OVERDENSE CLOUD

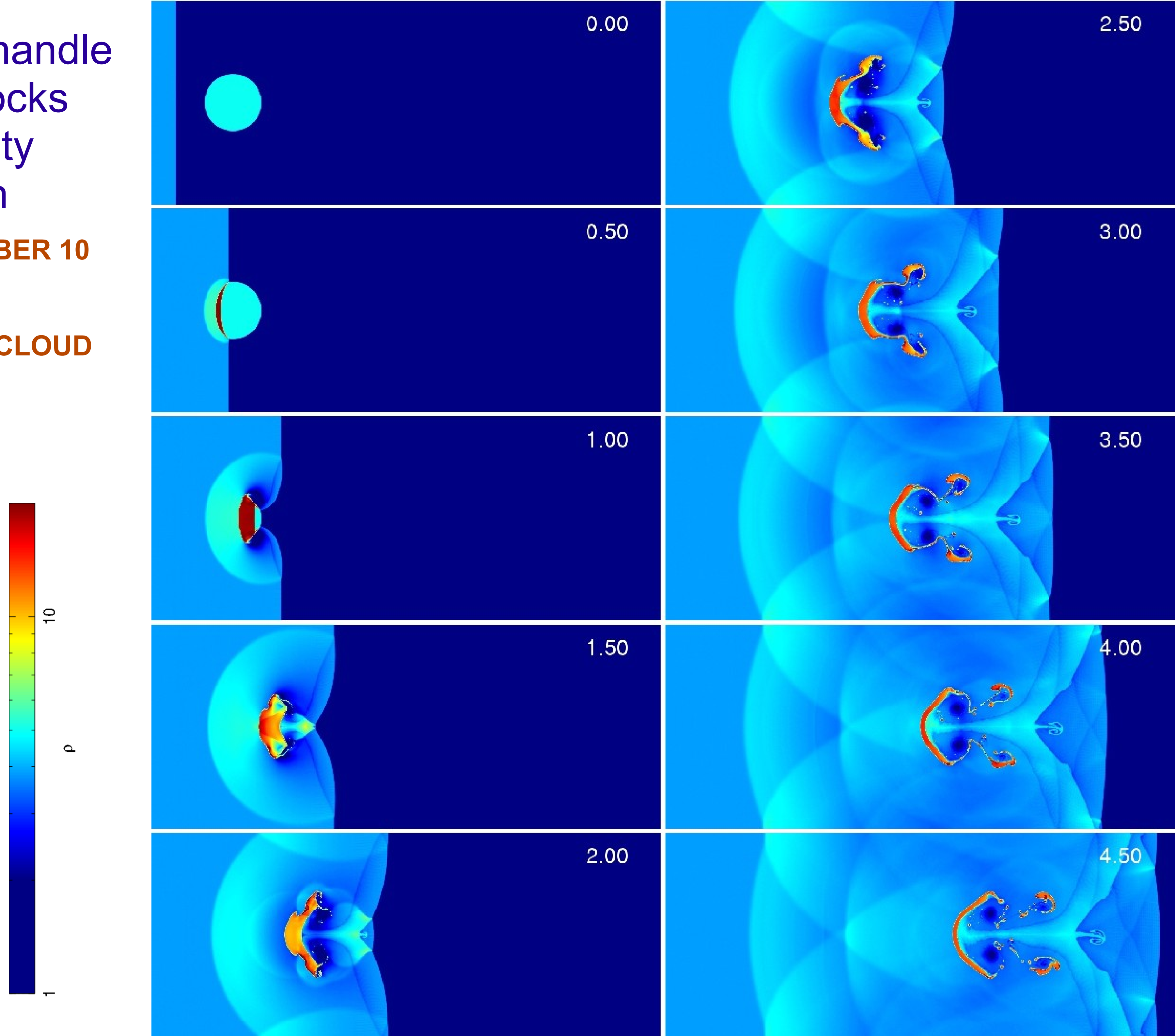

SPH accurately conserves all relevant conserved quantities in self-gravitating flows

SOME NICE PROPERTIES OF SPH

- ★ **Mass is conserved**
- ★ **Momentum is conserved**
- ★ **Total energy is conserved – also in the presence of self-gravity !**
- ★ **Angular momentum is conserved**
- ★ **Entropy is conserved – only produced by artificial viscosity, no entropy production due to mixing or advection**

Furthermore:

- ★ **High geometric flexibility**
- ★ **Easy incorporation of vacuum boundary conditions**
- ★ **No high Mach number problem**

The basic dynamics of structure formation in the **dark matter**

BASIC EQUATIONS AND THEIR DISCRETIZATION

Gravitation
(Newtonian approximation to GR in an expanding space-time)

Dark matter is collisionless

Monte-Carlo integration as **N-body System**

3N **coupled**, non-linear differential equations of second order

Friedmann-Lemaitre model

$$H(a) = H_0 \sqrt{a^{-3}\Omega_0 + a^{-2}(1 - \Omega_0 - \Omega_\Lambda) + \Omega_\Lambda}$$

Collisionless Boltzmann equation with self-gravity

$$\frac{\mathrm{d}f}{\mathrm{d}t} \equiv \frac{\partial f}{\partial t} + \mathbf{v}\frac{\partial f}{\partial \mathbf{x}} - \frac{\partial \Phi}{\partial \mathbf{r}}\frac{\partial f}{\partial \mathbf{v}} = 0$$

$$\nabla^2 \Phi(\mathbf{r}, t) = 4\pi G \int f(\mathbf{r}, \mathbf{v}, t)\mathrm{d}\mathbf{v}$$

Hamiltonian dynamics in expanding space-time

$$H = \sum_i \frac{\boldsymbol{p}_i^2}{2\, m_i\, a(t)^2} + \frac{1}{2}\sum_{ij} \frac{m_i m_j\, \varphi(\boldsymbol{x}_i - \boldsymbol{x}_j)}{a(t)}$$

$$\nabla^2 \varphi(\boldsymbol{x}) = 4\pi G \left[-\frac{1}{L^3} + \sum_{\boldsymbol{n}} \tilde{\delta}(\boldsymbol{x} - \boldsymbol{n}L) \right]$$

Problems:

- N ist very large
- All equations are coupled with each other

Non-radiative gasdynamics can be easily included in cosmological simulations

SIMULATED CLUSTER FORMATION WITH GAS

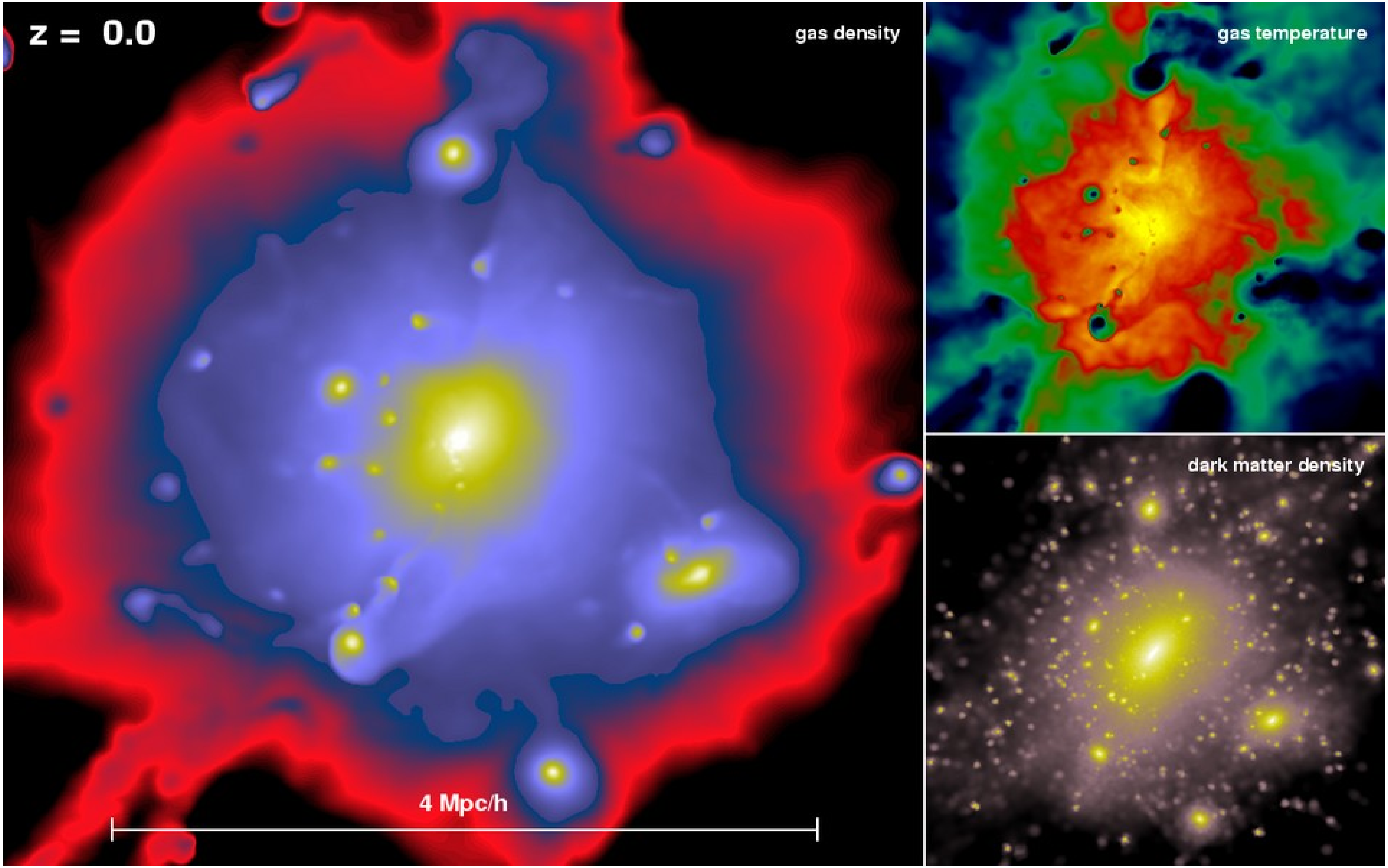

Supersonic motion creates shock waves

SHOCK WAVES OF A BULLET TRAVELLING IN AIR

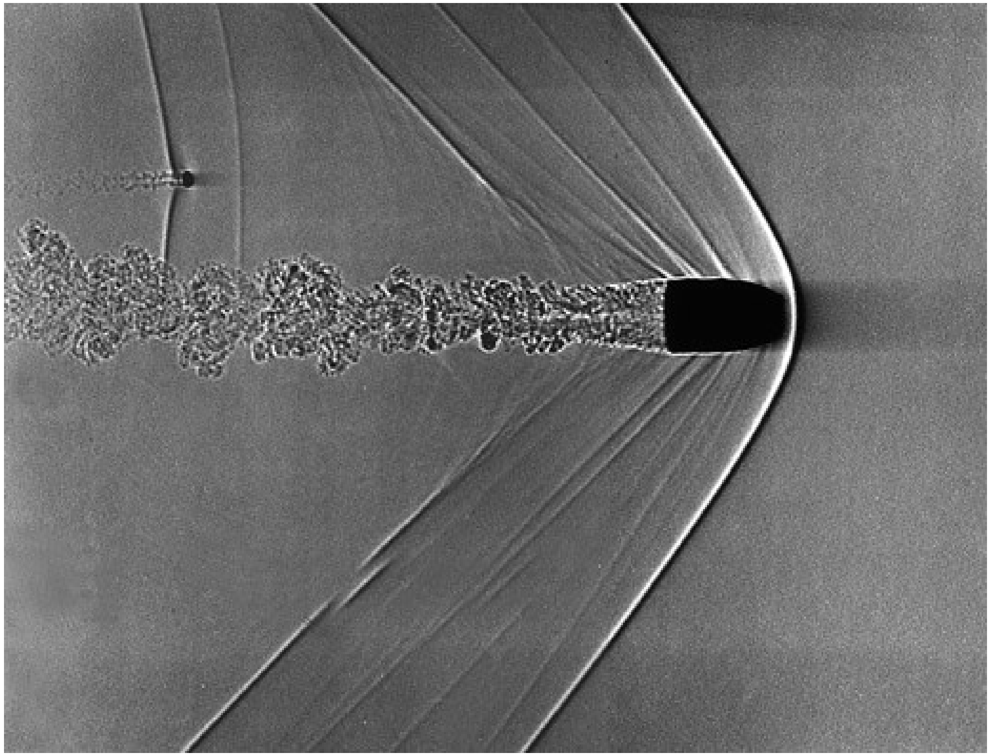

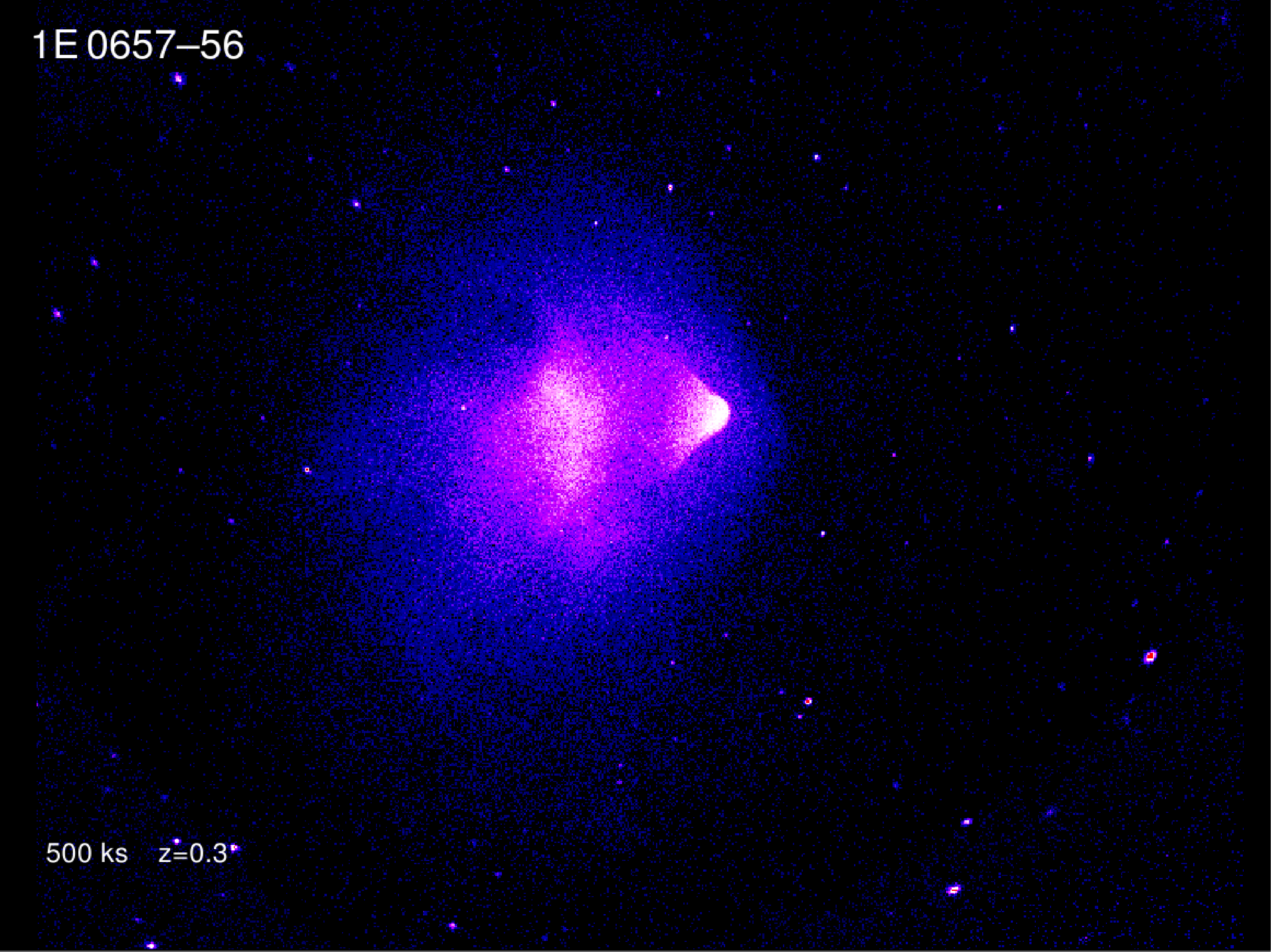
1E 0657−56
500 ks
z=0.3

Weak lensing mass reconstructions have confirmed an offset between mass peaks and X-ray emission

MASS CONTOURS FROM LENSING COMPARD TO X-RAY EMISSION

Clowe et al. (2006)

Magellan Optical Image

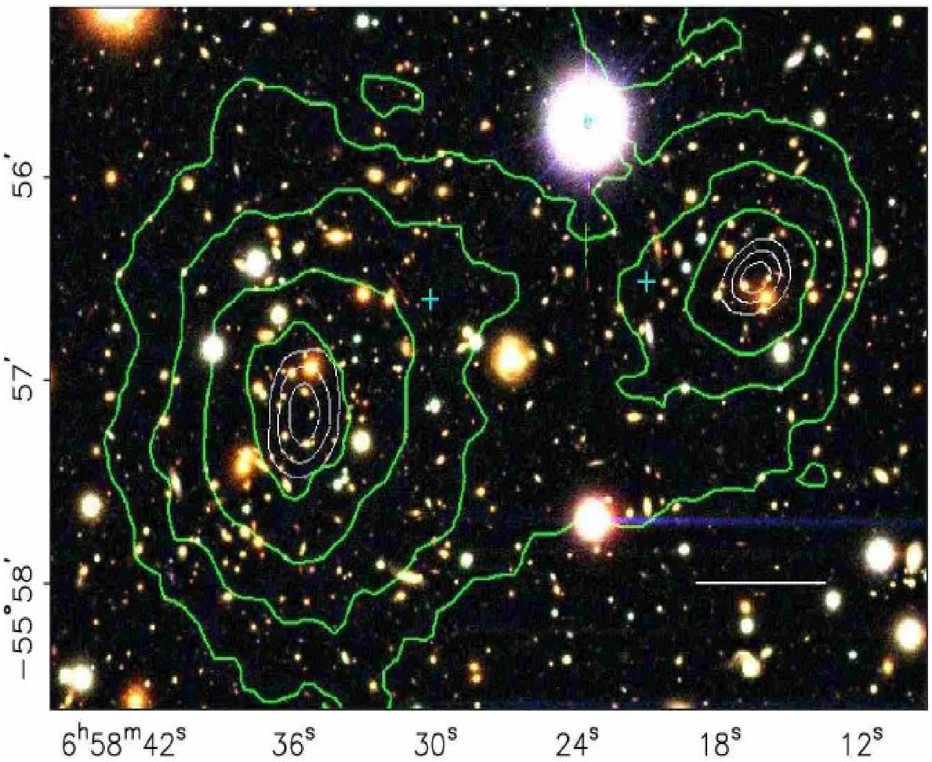

500 ksec Chandra exposure

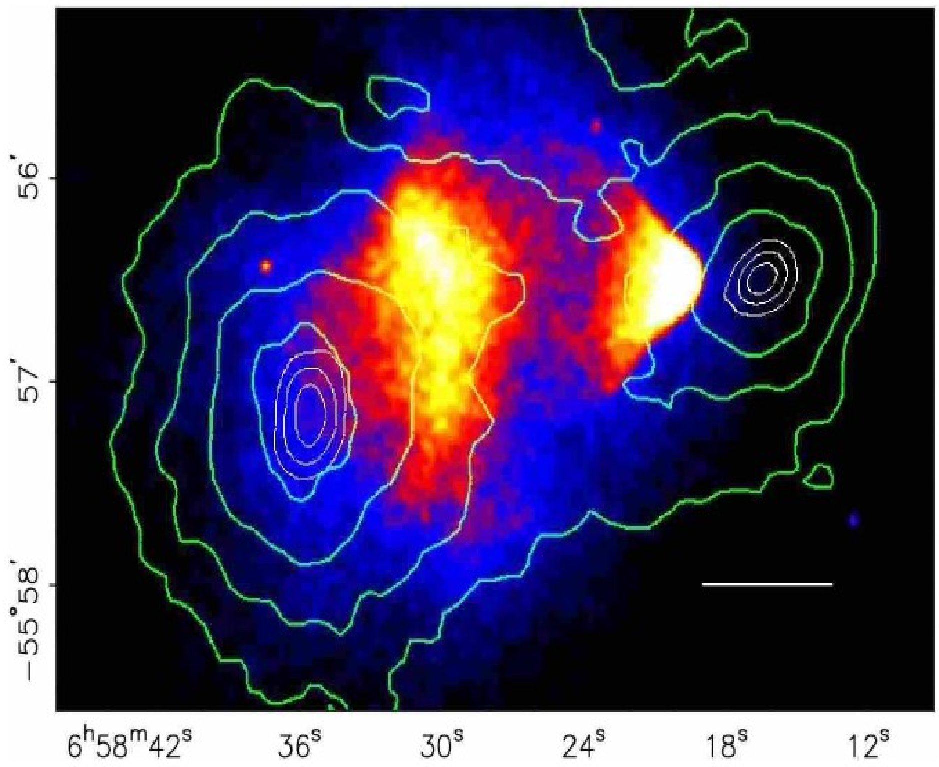

weak lensing mass contours overlaid

NASA Press Release Aug 21, 2006:

1E 0657-56: NASA Finds Direct Proof of Dark Matter

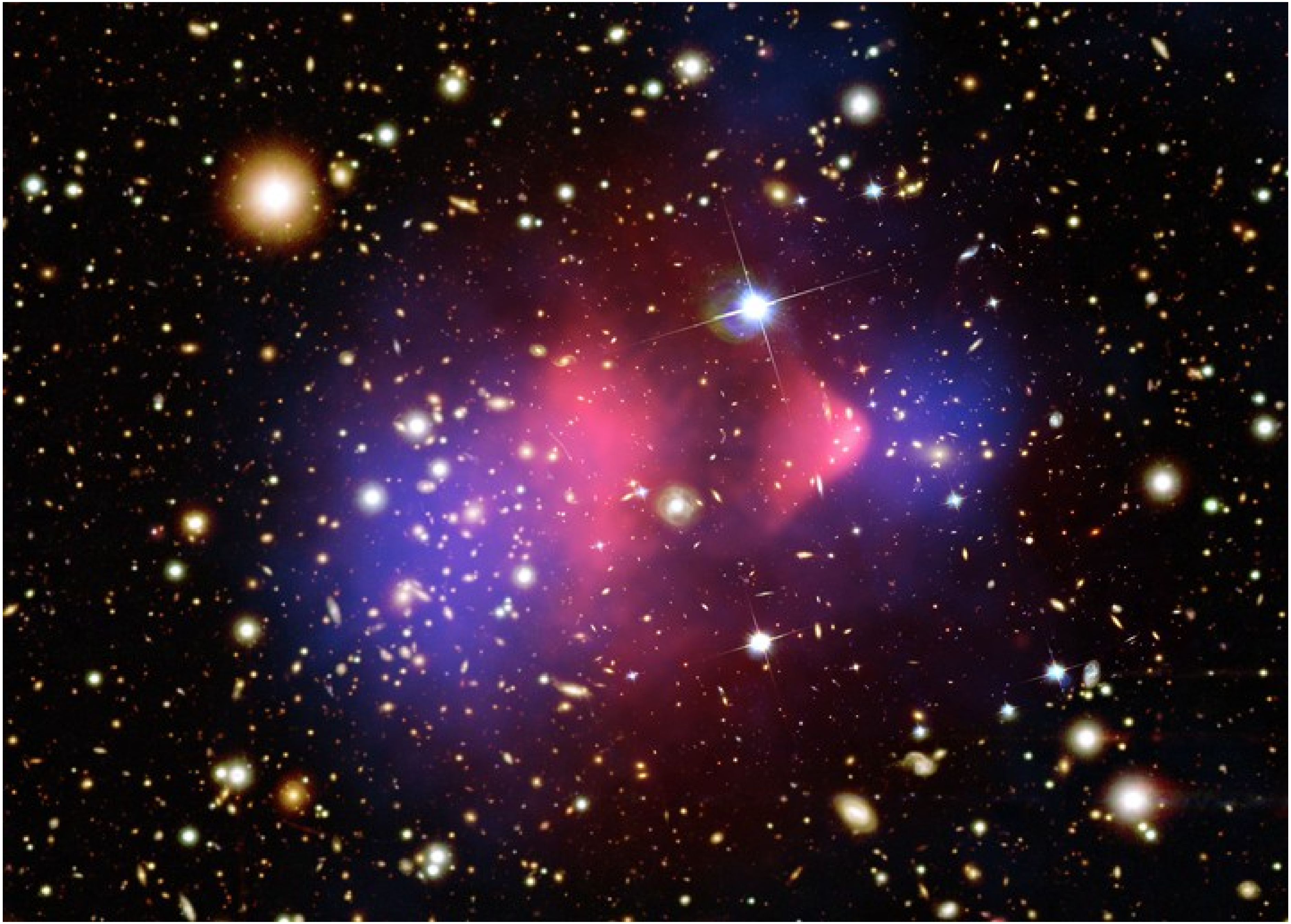

Fitting the density jump in the X-ray surface brightness profile allows a measurement of the shock's Mach number

X-RAY SURFACE BRIGHTNESS PROFILE

Markevitch et al. (2006)

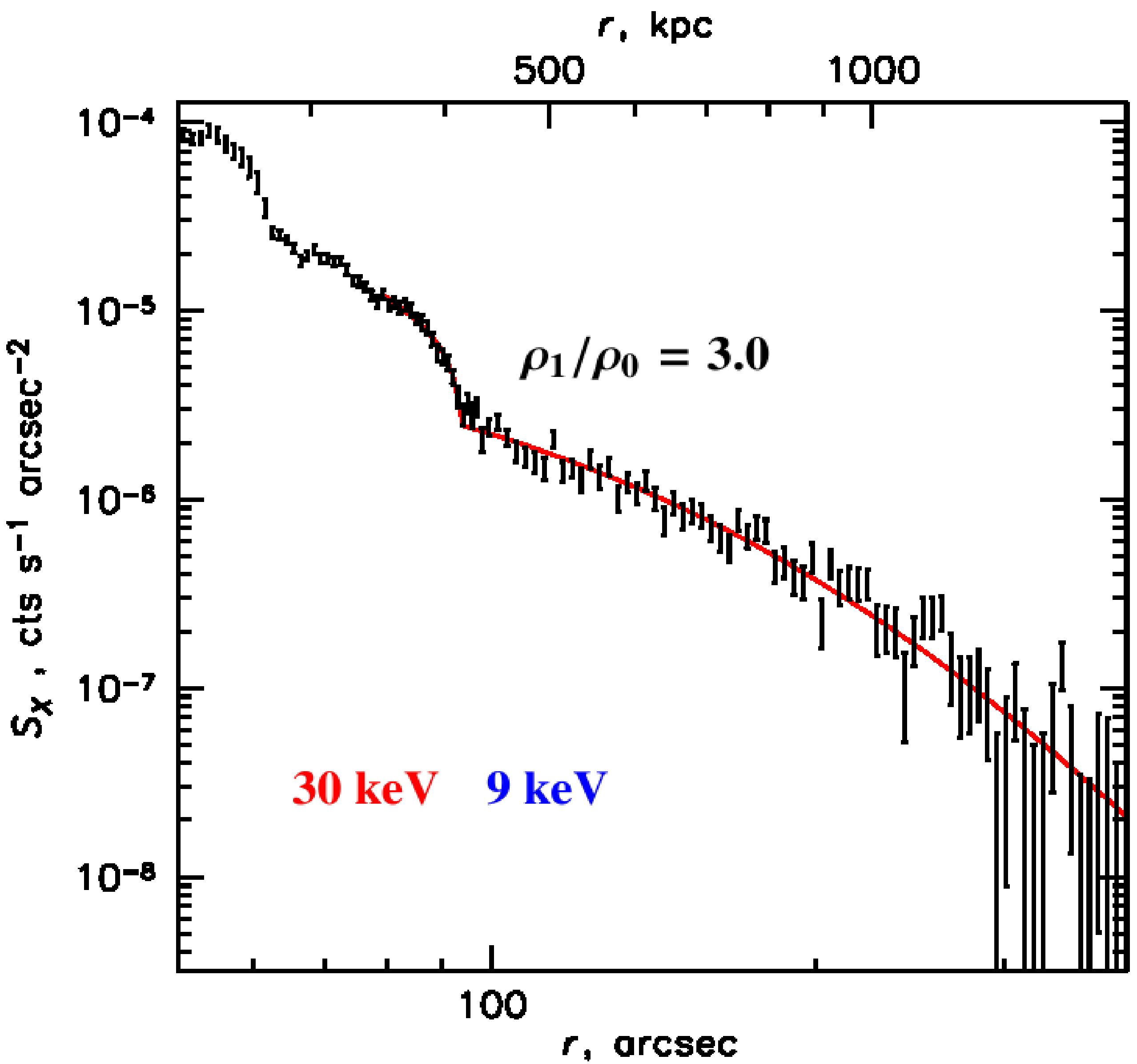

shock strength:

M = 3.0 ± 0.4

shock velocity:

v_s = 4700 km/s

Usually, shock velocity has been identified with velocity of the bullet.

How rare is the bullet cluster?

DISTRIBUTION OF VELOCITIES OF THE MOST MASSIVE SUBSTRUCTURE IN THE MILLENNIUM RUN

Hayashi & White (2006)

Adopted mass model from Clowe et al. (2004):

NFW-Halo with:

$M_{200} = 2.96 \times 10^{15}\ M_\odot$
$R_{200} = 2.25$ Mpc

$V_{200} = 2380$ km/sec
$V_{shock} = 4500$ km/sec

$V_{sub}/V_{shock} = 1.9$ chance: 10^{-2}

But, revised data from Clowe et al. (2006) and Markevitch el al. (2006):

$M_{200} = 1.5 \times 10^{15}\ M_\odot$

$V_{200} = 1680$ km/sec
$V_{shock} = 4740$ km/sec

$V_{sub}/V_{shock} = 2.8$ chance: 10^{-7}

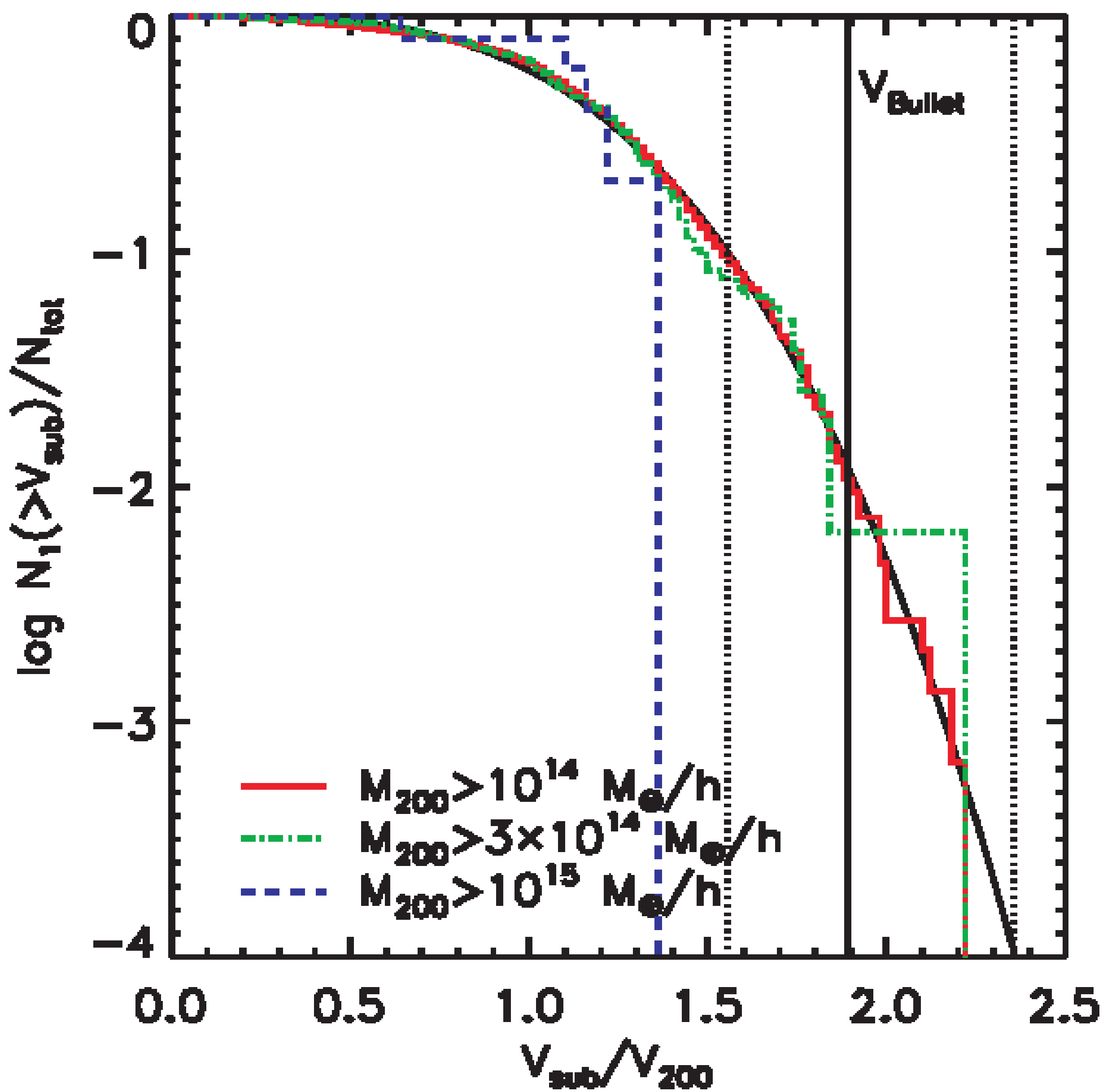

A simple toy merger model of two NFW halos on a zero-energy collision orbit

PARAMETERS OF A BASIC TOY MODEL

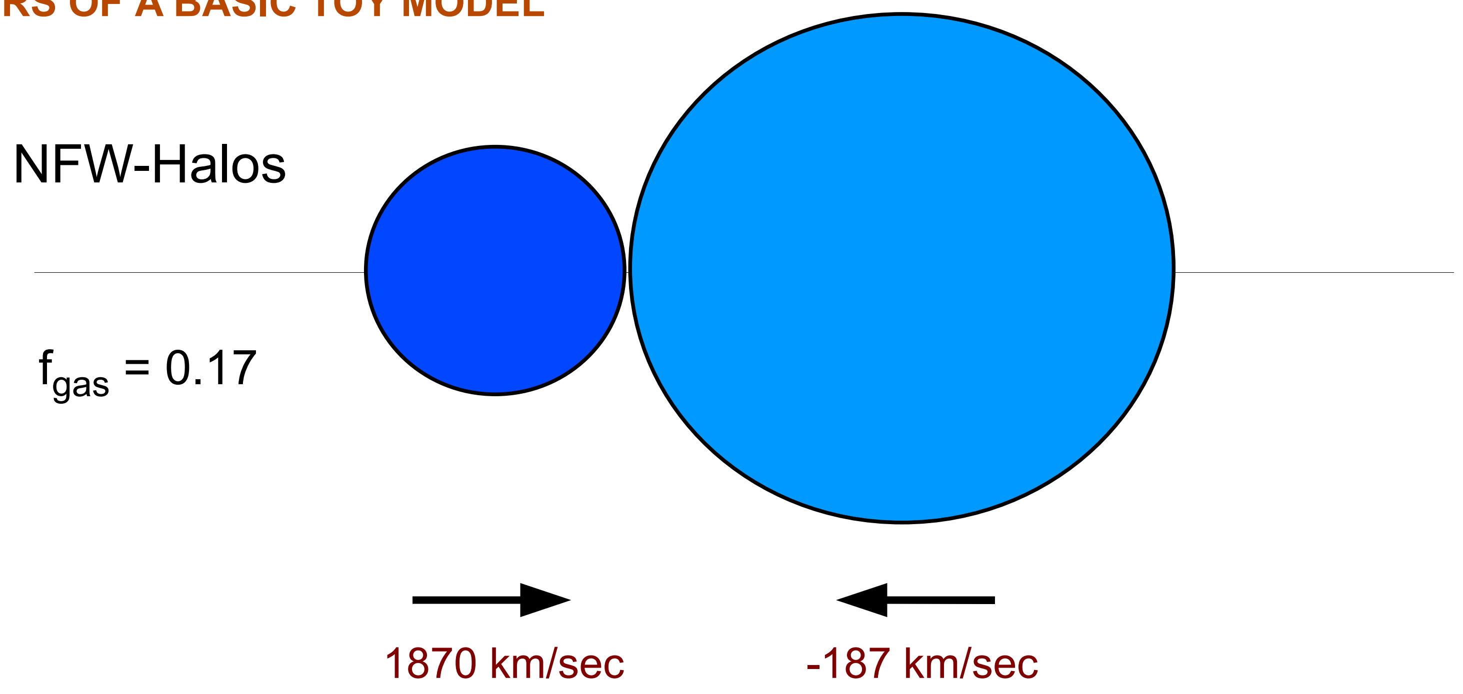

Mass model from Clowe et al. (2006):

$\mathbf{M_{200} = 1.5 \times 10^{14} M_\odot}$	$\mathbf{M_{200} = 1.5 \times 10^{15} M_\odot}$
R_{200} = 1.1 Mpc	R_{200} = 2.3 Mpc
c = 7.2	c = 2.0
V_{200} = 780 km/sec	V_{200} = 1680 km/sec

VIDEO OF THE TIME EVOLUTION OF A SIMPLE BULLET CLUSTER MODEL

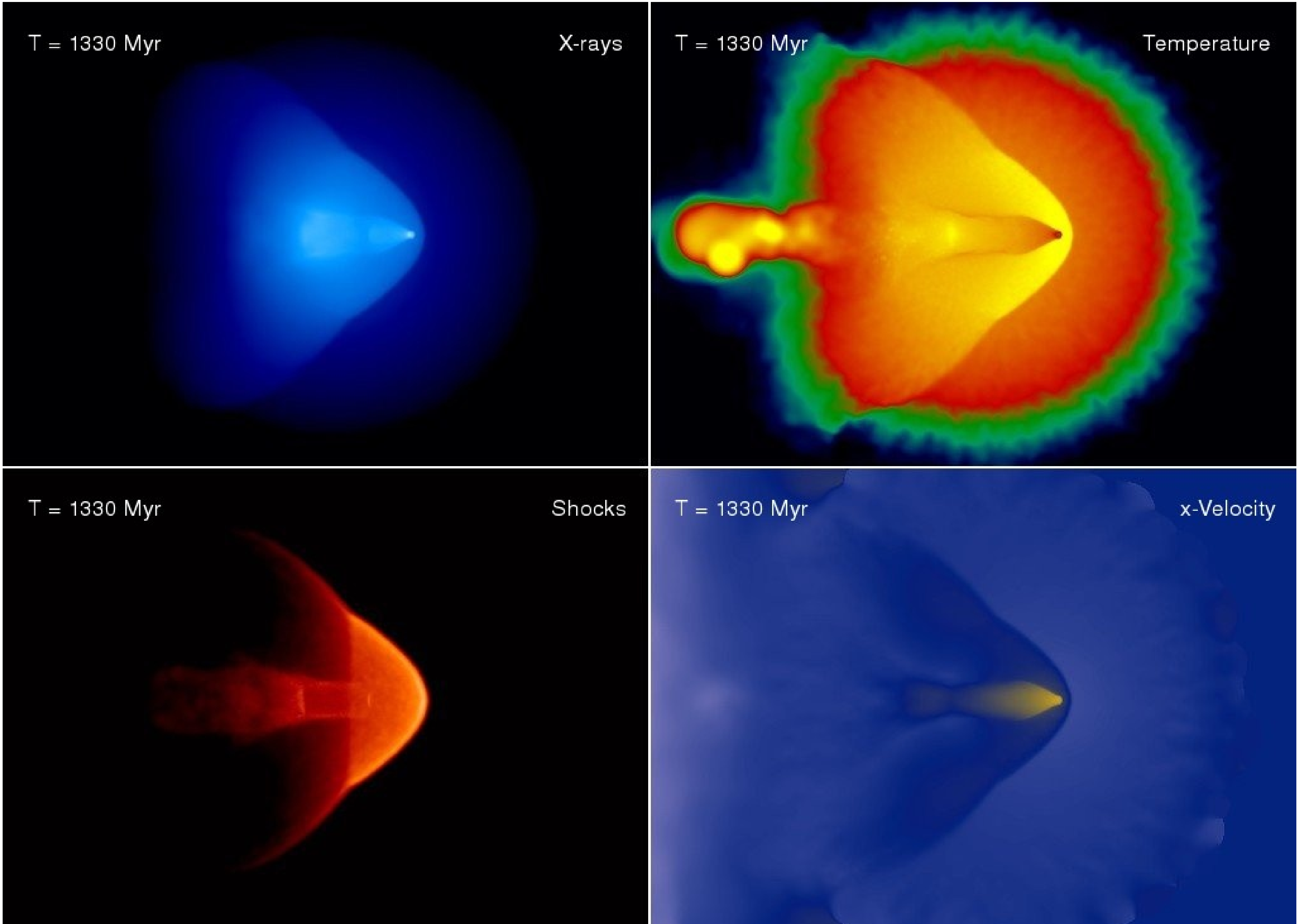

Drawing the observed X-ray map and the simulation images with the same color-scale simplifies the comparison

SIMULATED X-RAY MAP COMPARED TO OBSERVATION

Candra 500 ks image

bullet cluster simulation

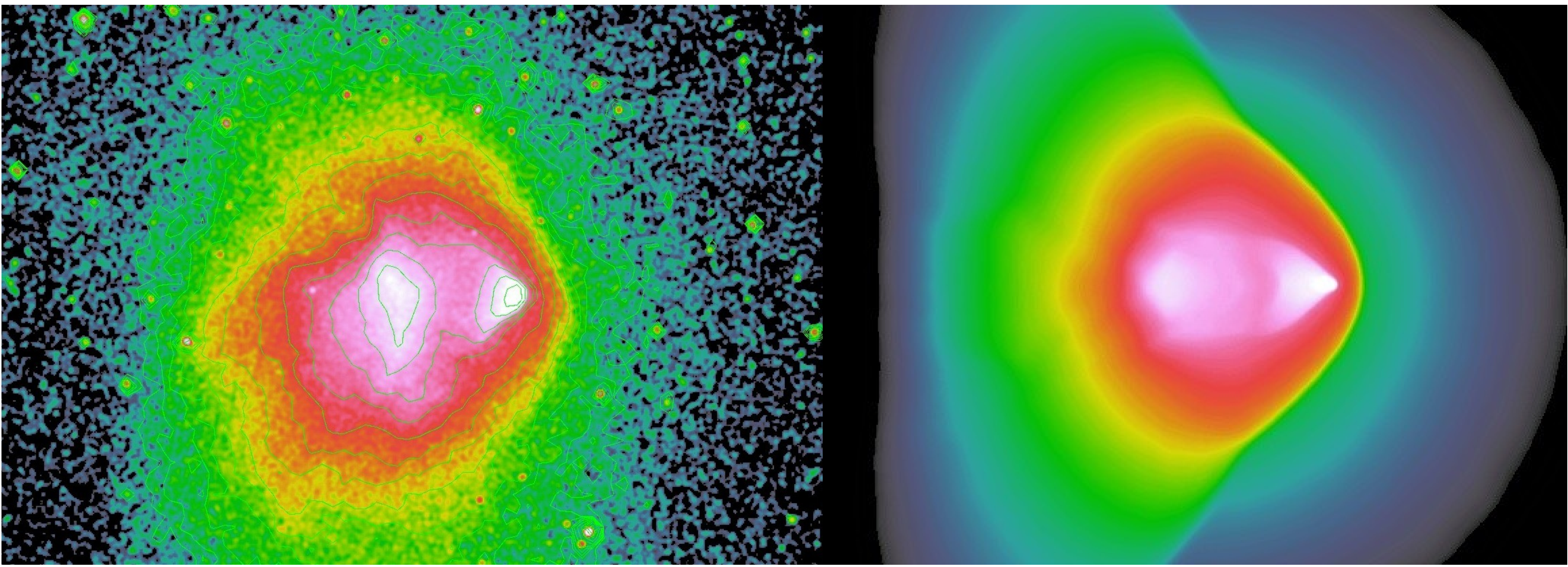

Springel & Farrar (2007)

The model also matches the observed temperature and mass profiles

COMPARISON OF SIMULATED TEMPERATURE AND MASS PROFILE WITH OBSERVATIONS

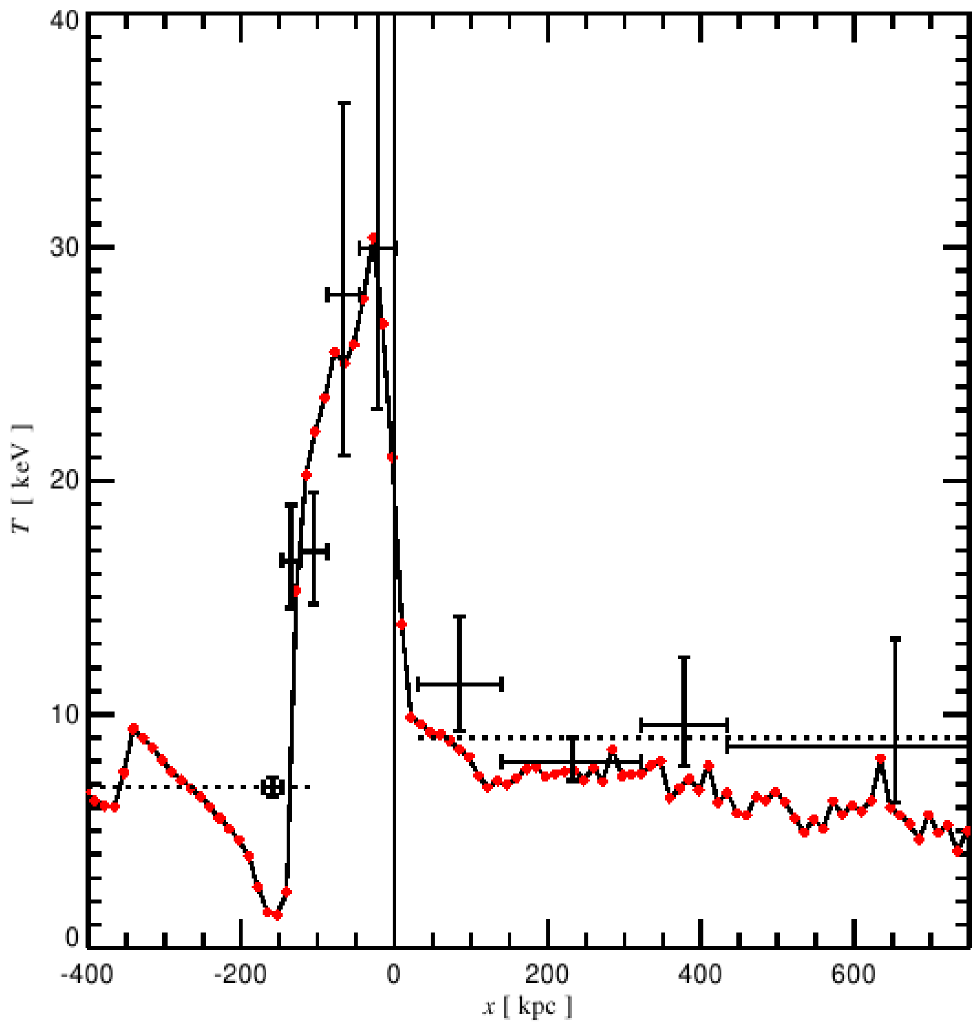

Data from **Markevitch et al. (2006)**

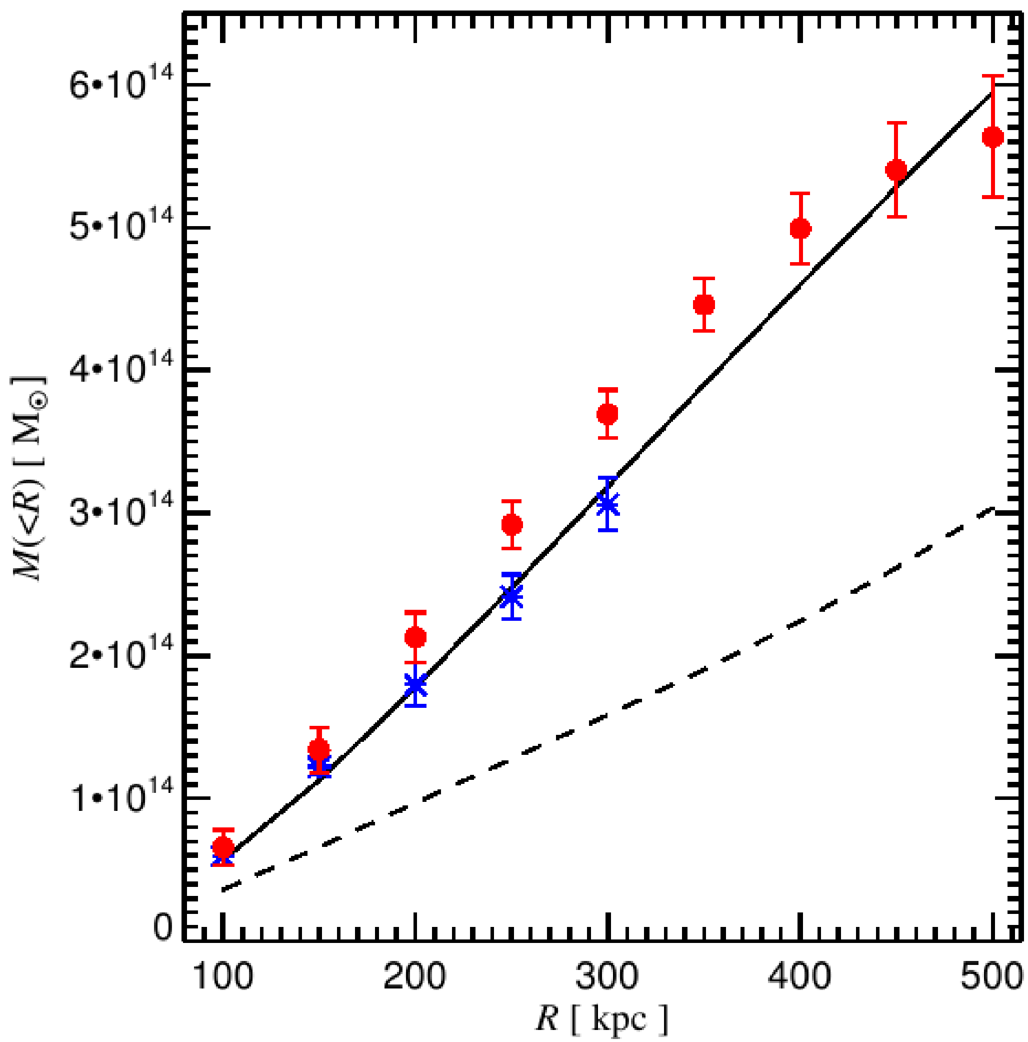

Data from **Bradac et al. (2006)**

Despite a shock speed of ~4500 km/s, the bullet moves considerably slower

VELOCITIES AND POSITIONS OF MAIN BULLET CLUSTER FEATURES AS A FUNCTION OF TIME

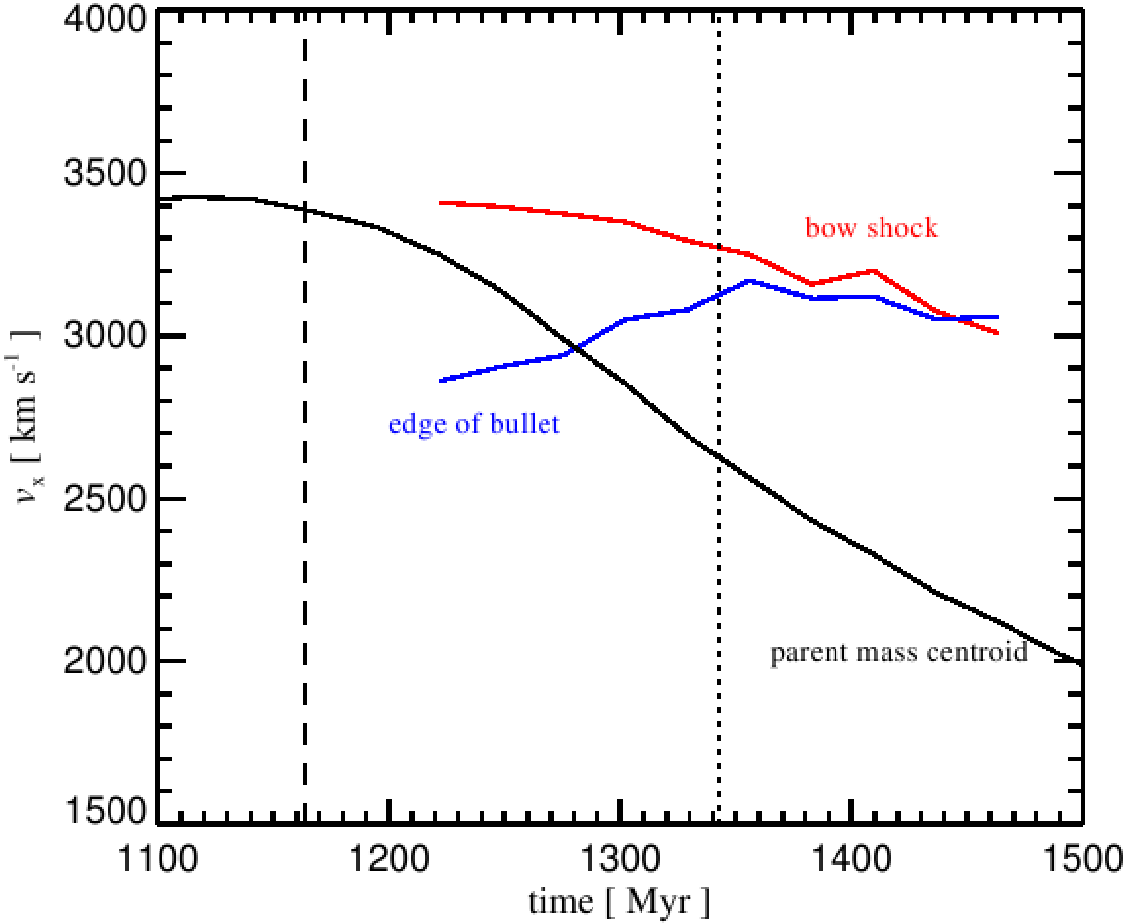

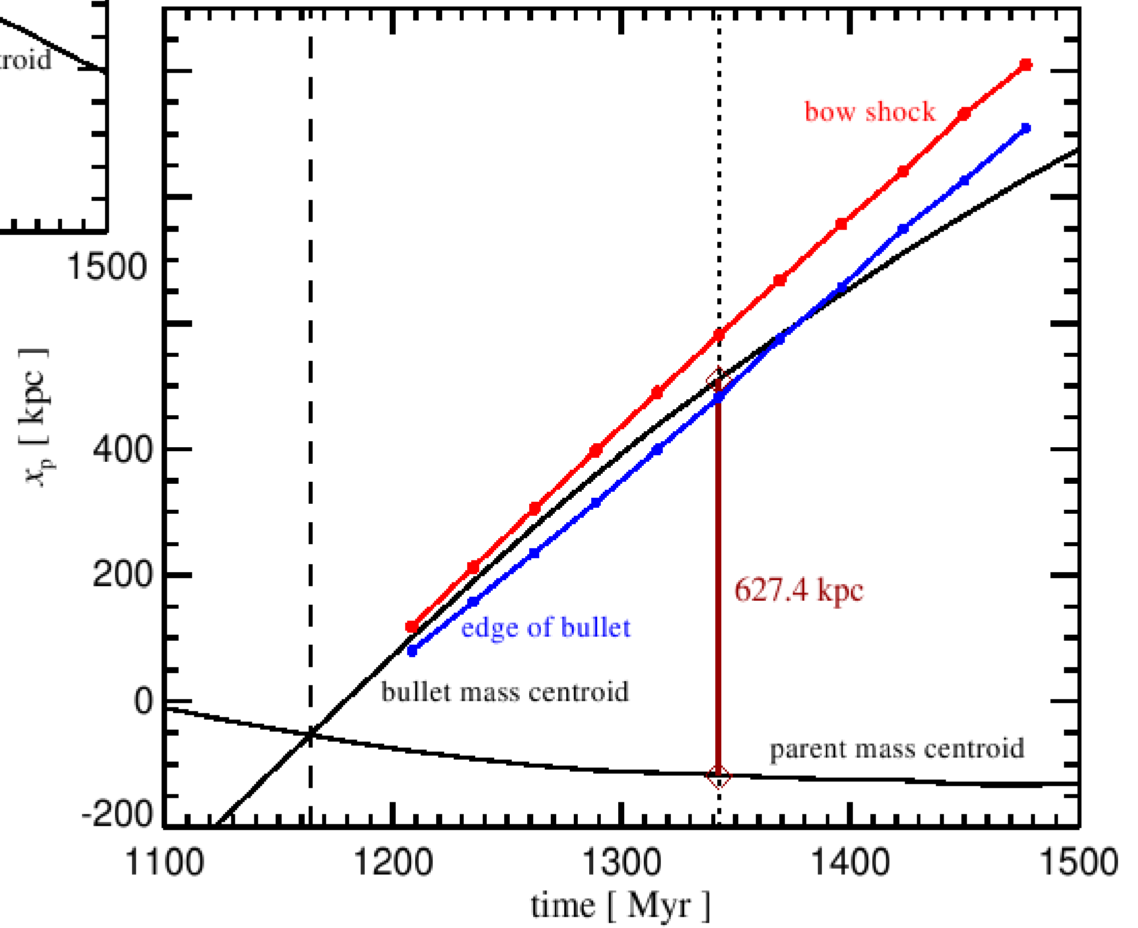

Shock speed: 4500 km/s

Pre-shock infall: -1100 km/s

Shock speed relative to bullet: -800 km/s

Speed of bullet: 2600 km/s

The challenge to simulate galaxy formation

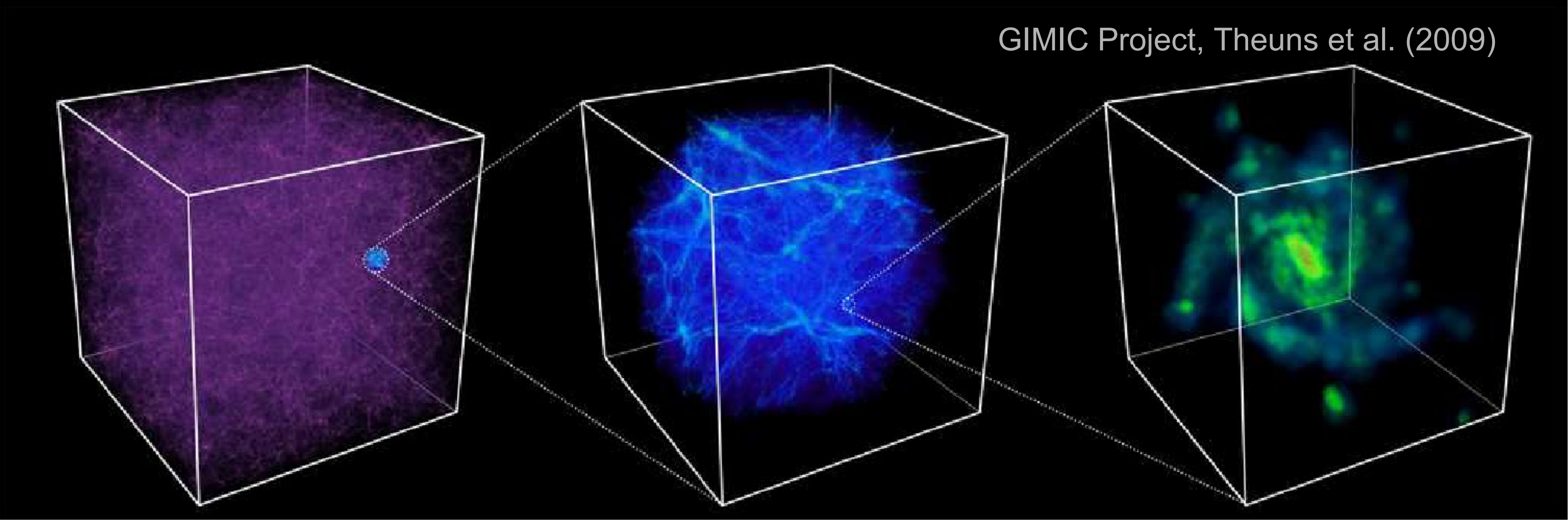

Hydrodynamical simulations aim to predict:

- **Morphology of galaxies**
- **Fate of the diffuse gas, WHIM, metal enrichment**
- **X-ray atmospheres in halos**
- **Turbulence in halos and accretion shocks**
- **Large-scale regulation of star formation in galaxies through feedback processes from stars and black holes**
- **Transport processes (e.g. conduction)**
- **Radiative transfer**
- **Dynamical transformations (e.g. ram-pressure stripping)**
- **Magnetic fields**

Feedback physics appears crucial for any successful model of dwarf galaxy formation

But what physics is responsible for low star formation in the first place?

- Correlated supernova explosions in starbursts
- Stellar winds and galactic winds
- Photoionization by a UV background
- AGN activity
- Radiation pressure
- Cosmic ray pressure
- Magnetic fields
- ISM turbulence
- Ram pressure stripping
- Gravitational tidal harassment, tidal truncation

SPH simulations have become an indispensable tool for studying this physics

The role of supermassive black holes

In major-mergers between two disk galaxies, tidal torques extract angular momentum from cold gas, providing fuel for nuclear starbursts

TIME EVOLUTION OF A PROGRADE MAJOR MERGER

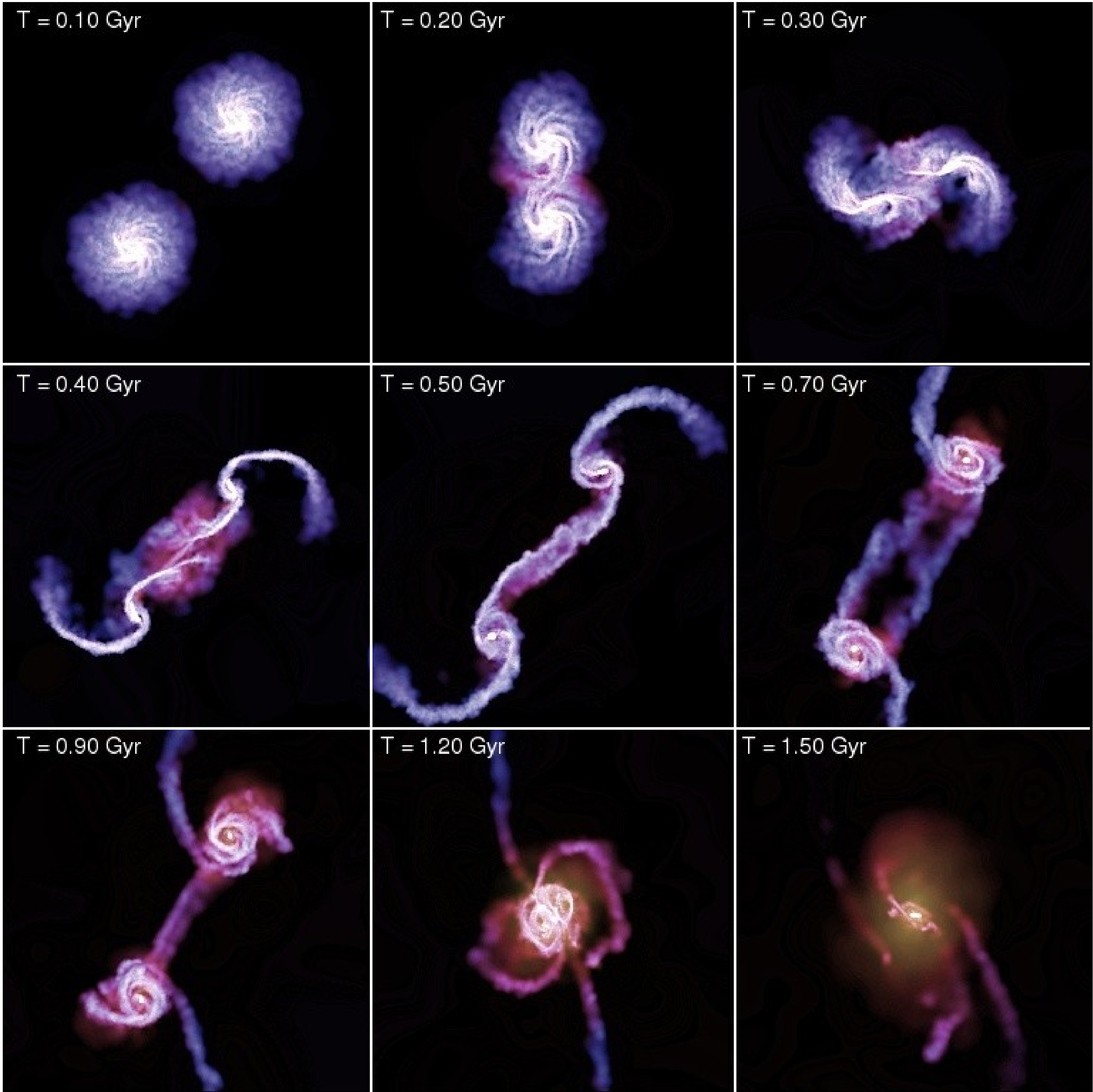

Thermal conduction

Thermal conduction may partially offset radiative cooling in central cluster regions

THE CONDUCTION IDEA

Inner region of clusters (~10-50 kpc) is cooler than the rest of the cluster → Is thermal conduction from the outer hot regions of the cluster the heat source?

Zakamska & Narayan (2003)

- Assume hydrostatic equilibrium with a balance between cooling and conductive heating
- Temperature profiles of five clusters can be well fit, requiring conductives of the order 30% Spitzer-value

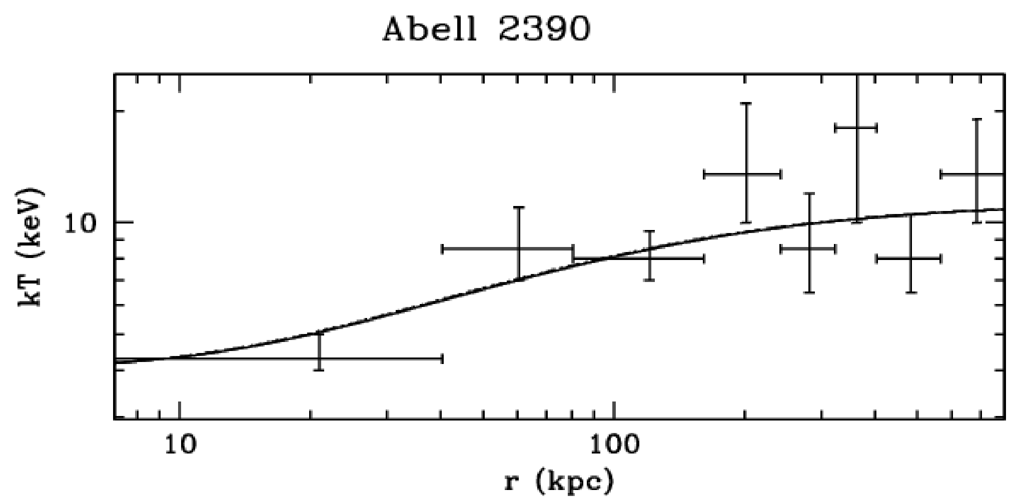

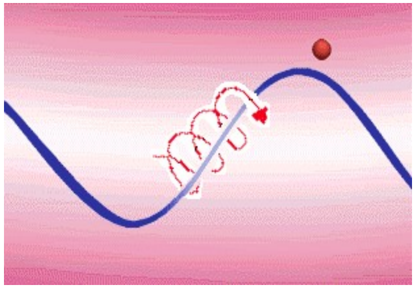

BUT: Magnetic fields are the natural enemy of conduction....

A robust and accurate implementation of thermal conduction in SPH

SPH DISCRETIZATION OF CONDUCTION

Conduction equation:

$$\mathbf{j} = -\kappa \nabla T$$

$$\rho \frac{\mathrm{d}u}{\mathrm{d}t} = -\nabla \mathbf{j}$$

$$\frac{\mathrm{d}u}{\mathrm{d}t} = \frac{1}{\rho} \nabla (\kappa \nabla T)$$

Second-order derivative tends to be noisy...

SPH discretization:

$$\frac{\mathrm{d}u_i}{\mathrm{d}t} = \sum_j \frac{m_j}{\rho_i \rho_j} \frac{(\kappa_j + \kappa_i)\,(T_j - T_i)}{|\mathbf{x}_{ij}|^2} \mathbf{x}_{ij} \nabla_i W_{ij}$$

Brookshaw (1985)

Problems encountered in practice:

- Explicit time integration can easily lead to instabilities
- Individual timestepping may easily lead to errors in energy conservation (conductivity depends strongly on temperature)

→ Best solved with implicit **time integration** schemes, which guarantee robustness

Self-consistent cosmologicals simulations of cluster formation can be used to study the impact of conduction on the ICM

X-RAY AND TEMPERATURE MAPS

Coma-sized cluster, $M_{vir} \sim 10^{15}\ M_{\odot}$, adiabatic hydrodynamics

Gas density (X-rays)

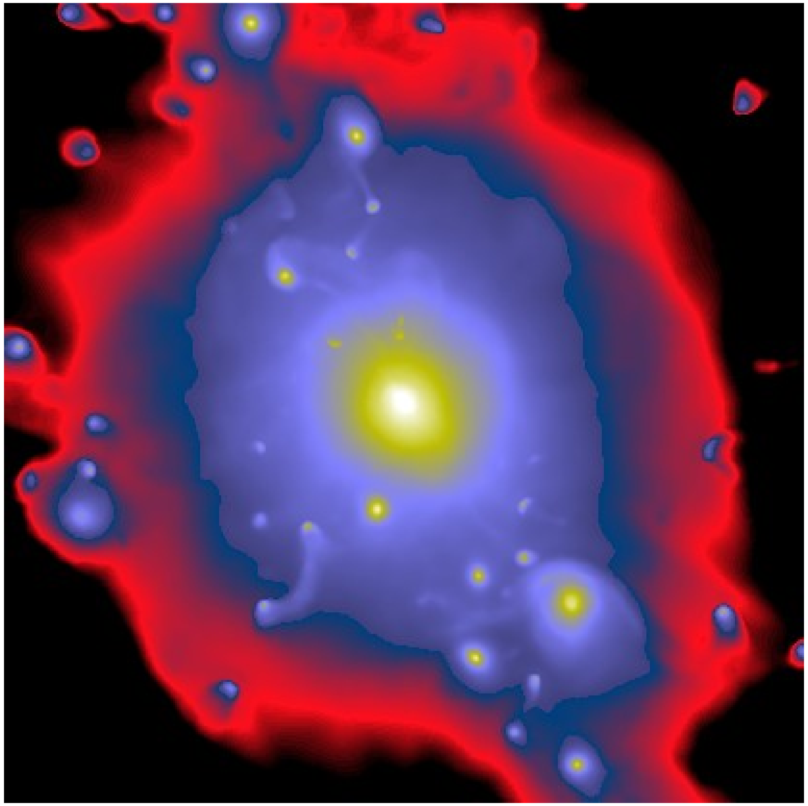

Mass-weighted temperature

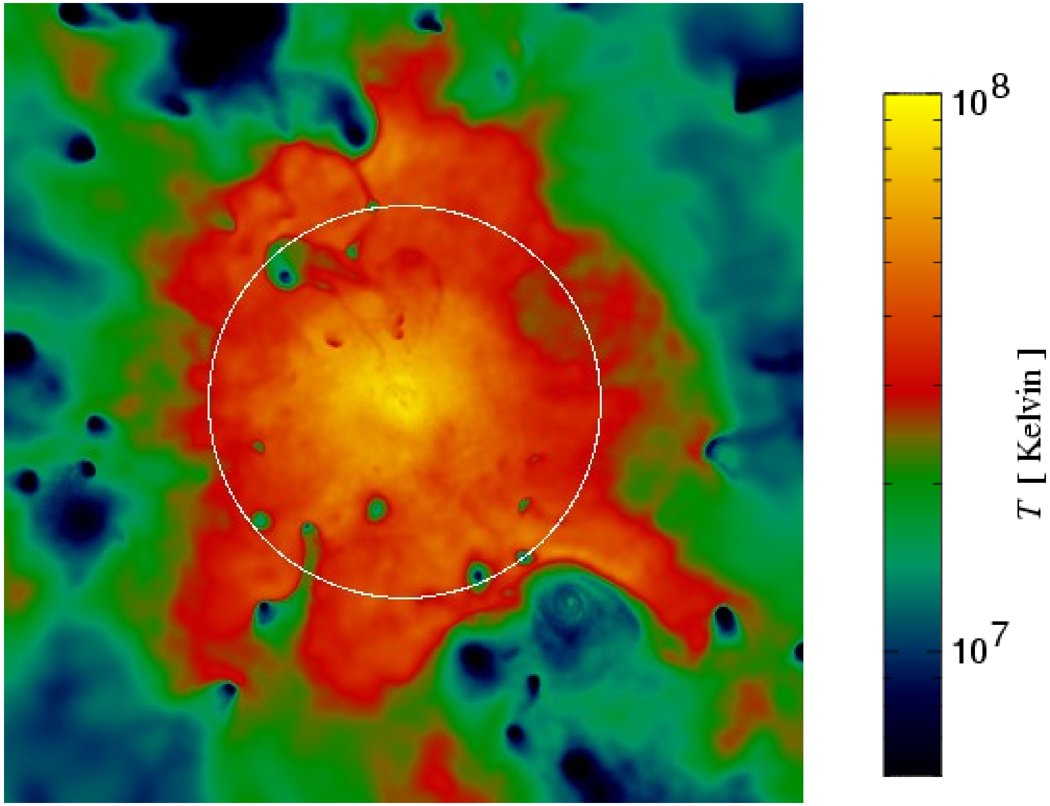

Thermal conduction near the Spitzer value strongly affects rich clusters of galaxies

X-RAY AND TEMPERATURE MAPS

Coma-sized cluster, $M_{vir} \sim 10^{15}\ M_{\odot}$,
adiabatic hydrodynamics, **thermal condution with $\kappa = \kappa_{sp}$**

Gas density (X-rays)

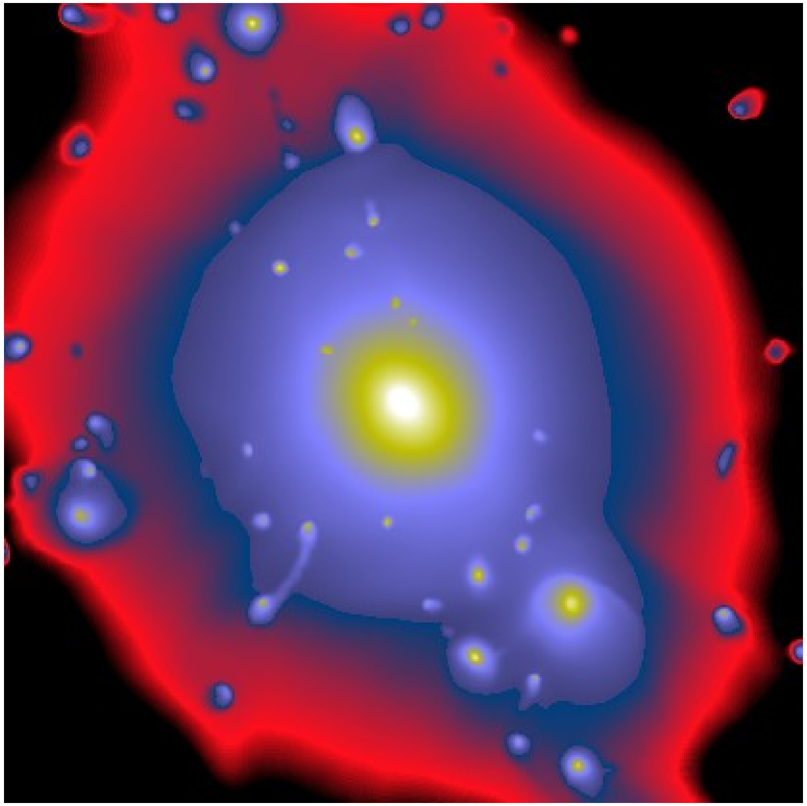

Mass-weighted temperature

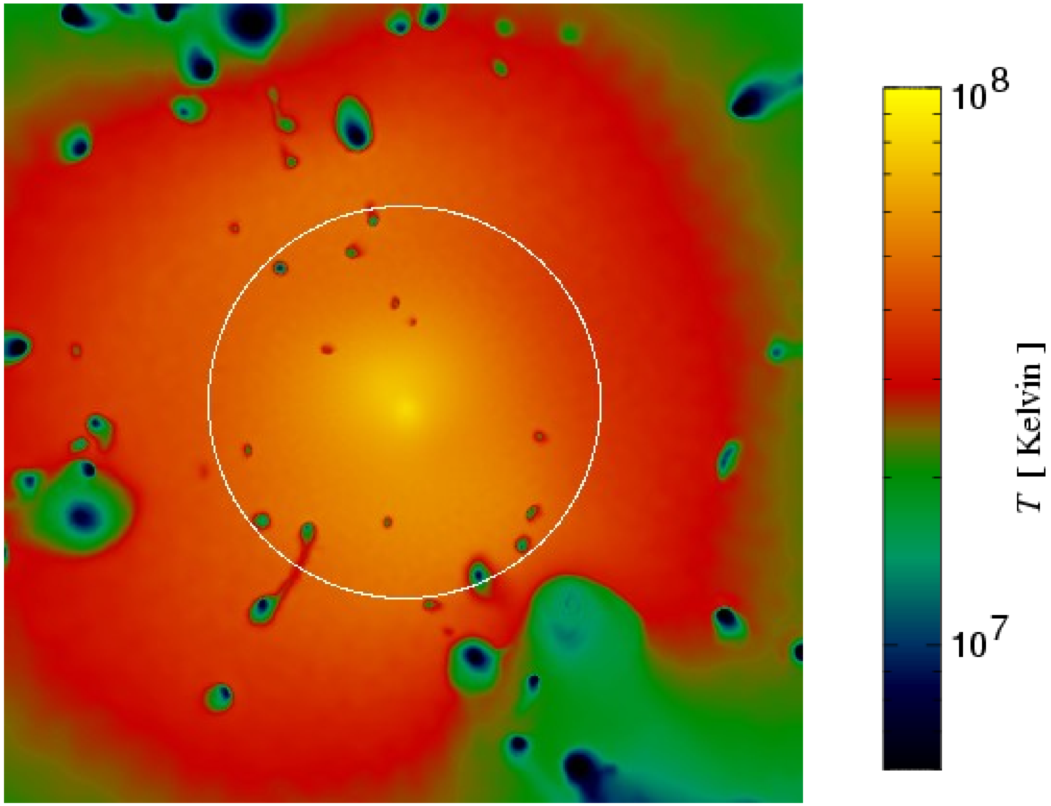

Physical viscosity in SPH

One can also derive an SPH discretization of the Navier-Stokes equations

SPH WITH PHYSICAL VISCOUS STRESSES

Viscous stresses modify the momentum flux density tensor: $\Pi_{ik} = p\delta_{ik} + \rho v_i v_k - \sigma_{ik}$

The stress tensor can be written as:

$$\sigma_{ik} = \eta \left(\frac{\partial v_i}{\partial x_k} + \frac{\partial v_k}{\partial x_i} - \frac{2}{3}\delta_{ik}\frac{\partial v_l}{\partial x_l} \right) + \zeta \delta_{ik} \frac{\partial v_l}{\partial x_l}$$

Shear viscosity coefficient (η)

Bulk viscosity coefficient (ζ)

The Euler equation of ideal gas dynamics is then replaced by the **Navier Stokes equations**:

$$\rho \left(\frac{\partial v_i}{\partial t} + v_k \frac{\partial v_i}{\partial x_k} \right) = -\frac{\partial p}{\partial x_i} - \rho \frac{\partial \Phi}{\partial x_i} + \frac{\partial}{\partial x_k}\left[\eta \left(\frac{\partial v_i}{\partial x_k} + \frac{\partial v_k}{\partial x_i} - \frac{2}{3}\delta_{ik}\frac{\partial v_l}{\partial x_l} \right) \right] + \frac{\partial}{\partial x_i}\left(\zeta \frac{\partial v_l}{\partial x_l} \right)$$

If conduction is also included, the thermal energy equation becomes the **generalized heat transfer equation:**

$$\rho T \frac{\mathrm{d}S}{\mathrm{d}t} = \nabla(\kappa \nabla T) + \frac{1}{2}\eta\, \sigma_{\alpha\beta}\sigma_{\alpha\beta} + \zeta (\nabla v)^2$$

SPH discretization of the Navier-Stokes equations

SPH WITH PHYSICAL VISCOUS STRESSES

Viscous flow between two plates

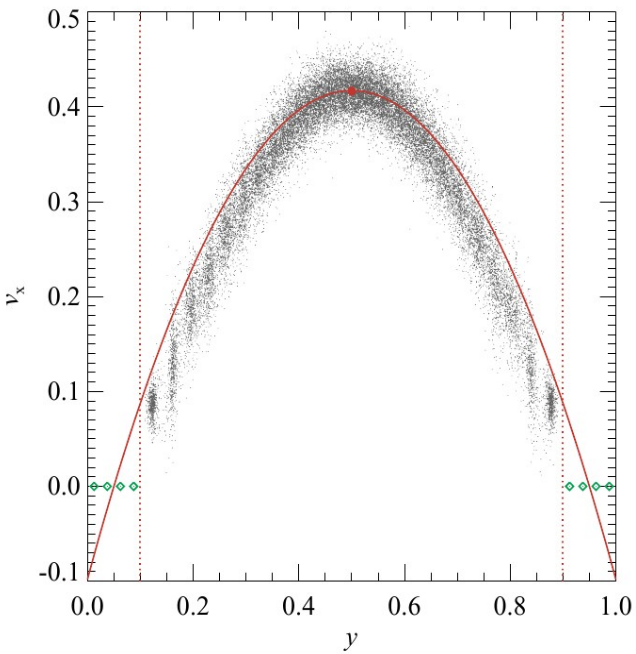

$$\left.\frac{\partial v_\alpha}{\partial x_\beta}\right|_i = \frac{1}{\rho_i}\sum_{j=1}^{N} m_j (\boldsymbol{v_j} - \boldsymbol{v_i})|_\alpha \, [\nabla_i W_{ij}(h_i)]|_\beta$$

$$\left.\sigma_{\alpha\beta}\right|_i = \eta\left(\left.\frac{\partial v_\alpha}{\partial x_\beta}\right|_i + \left.\frac{\partial v_\beta}{\partial x_\alpha}\right|_i - \frac{2}{3}\delta_{\alpha\beta}\left.\frac{\partial v_\gamma}{\partial x_\gamma}\right|_i\right) + \zeta\,\delta_{\alpha\beta}\left.\frac{\partial v_\gamma}{\partial x_\gamma}\right|_i$$

$$\left.\frac{\mathrm{d}v_\alpha}{\mathrm{d}t}\right|_{i,\mathrm{shear}} = \sum_{j=1}^{N} m_j \left[\frac{\eta_i \sigma_{\alpha\beta}|_i}{\rho_i^2}[\nabla_i W_{ij}(h_i)]|_\beta + \frac{\eta_j \sigma_{\alpha\beta}|_j}{\rho_j^2}[\nabla_i W_{ij}(h_j)]|_\beta\right]$$

$$\left.\frac{\mathrm{d}\boldsymbol{v}}{\mathrm{d}t}\right|_{i,\mathrm{bulk}} = \sum_{j=1}^{N} m_j \left[\frac{\zeta_i\, \nabla\cdot\boldsymbol{v}_i}{\rho_i^2}\nabla_i W_{ij}(h_i) + \frac{\zeta_j\, \nabla\cdot\boldsymbol{v}_j}{\rho_j^2}\nabla_i W_{ij}(h_j)\right]$$

$$\left.\frac{\mathrm{d}A_i}{\mathrm{d}t}\right|_{\mathrm{shear}} = \frac{1}{2}\,\frac{\gamma-1}{\rho_i^{\gamma-1}}\,\frac{\eta_i}{\rho_i}\,\sigma_i^2$$

$$\left.\frac{\mathrm{d}A_i}{\mathrm{d}t}\right|_{\mathrm{bulk}} = \frac{\gamma-1}{\rho_i^{\gamma-1}}\,\frac{\zeta_i}{\rho_i}\,(\nabla\cdot\boldsymbol{v}_i)^2$$

Sijacki & Springel (2006)

Viscous shear changes gas stripping during cluster assembly

COMPARISON OF PROJECTED GAS DENSITY MAPS

Sijacki & Springel (2006)

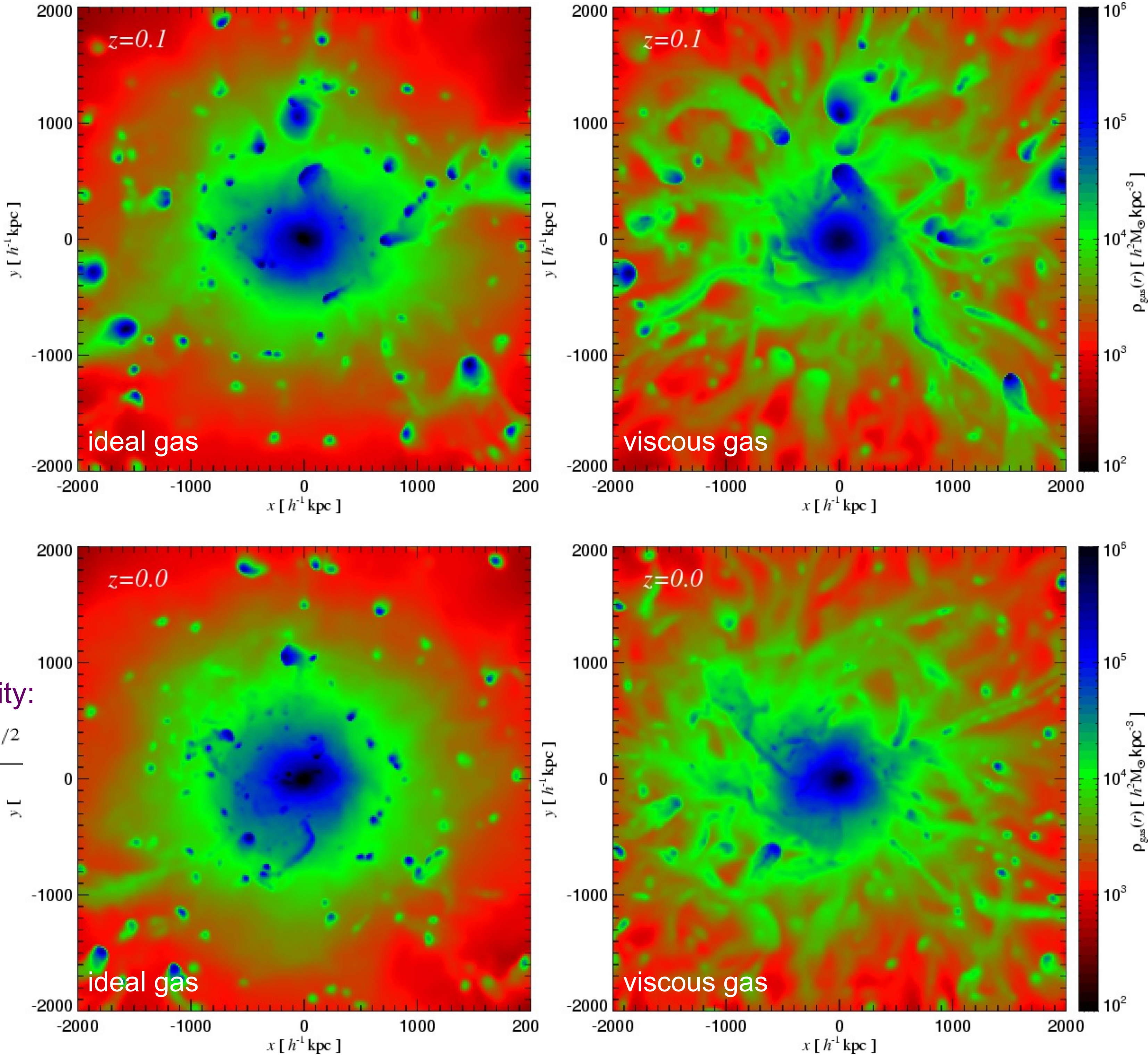

Braginskii shear viscosity:

$$\eta = 0.406 \frac{m_i^{1/2} (k_B T_i)^{5/2}}{(Ze)^4 \ln \Lambda}$$

Magnetic fields in SPH

It is possible to treat MHD in SPH, but divB errors remain problematic in the formulations proposed thus far

SPH MHD FORMULATIONS

Price & Monaghan (2005)
Dolag & Stasyszyn (2009)

(1) Direct discretization of the MHD equations in terms of *B*

Even when div B = 0 initially, the errors usually blow up when the magnetic forces become comparable to thermal pressure forces.

This needs to be controlled by field cleaning and/or smoothing methods, and a judicious choice of the SPH discretization.

(2) Use of the Euler potentials

$$\boldsymbol{B} = \nabla\alpha \times \nabla\beta$$

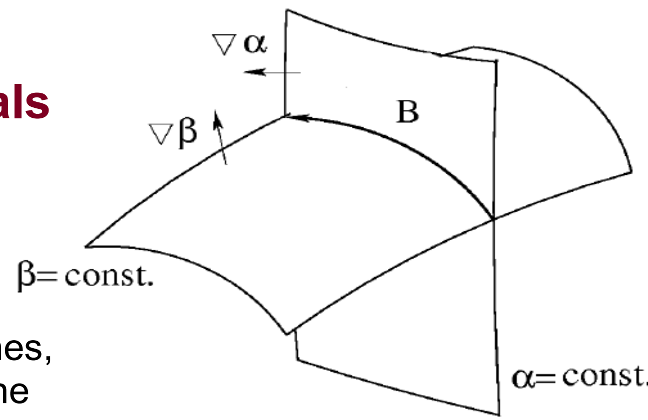

α and β effectively label field lines, and are simply advected with the flow in ideal MHD.

$$\frac{d\alpha_a}{dt} = 0 \qquad \frac{d\beta_a}{dt} = 0$$

Rosswog & Price (2008)

- Euler potentials not unique for a given field, and not all fields can be represented
- Unclear how dissipation should be treated
- Higher-order derivatives give noisy magnetic forces
- Dynamo action and magnetohydrodynamic turbulence may be suppressed (Brandenburg 2009)

(3) Use of the vector potential?

How well does (standard) SPH work?

SPH convergence rate for acoustic waves

ERROR NORM FOR THE VELOCITY AS A FUNCTION OF RESOLUTION (DISABLED VISCOSITY)

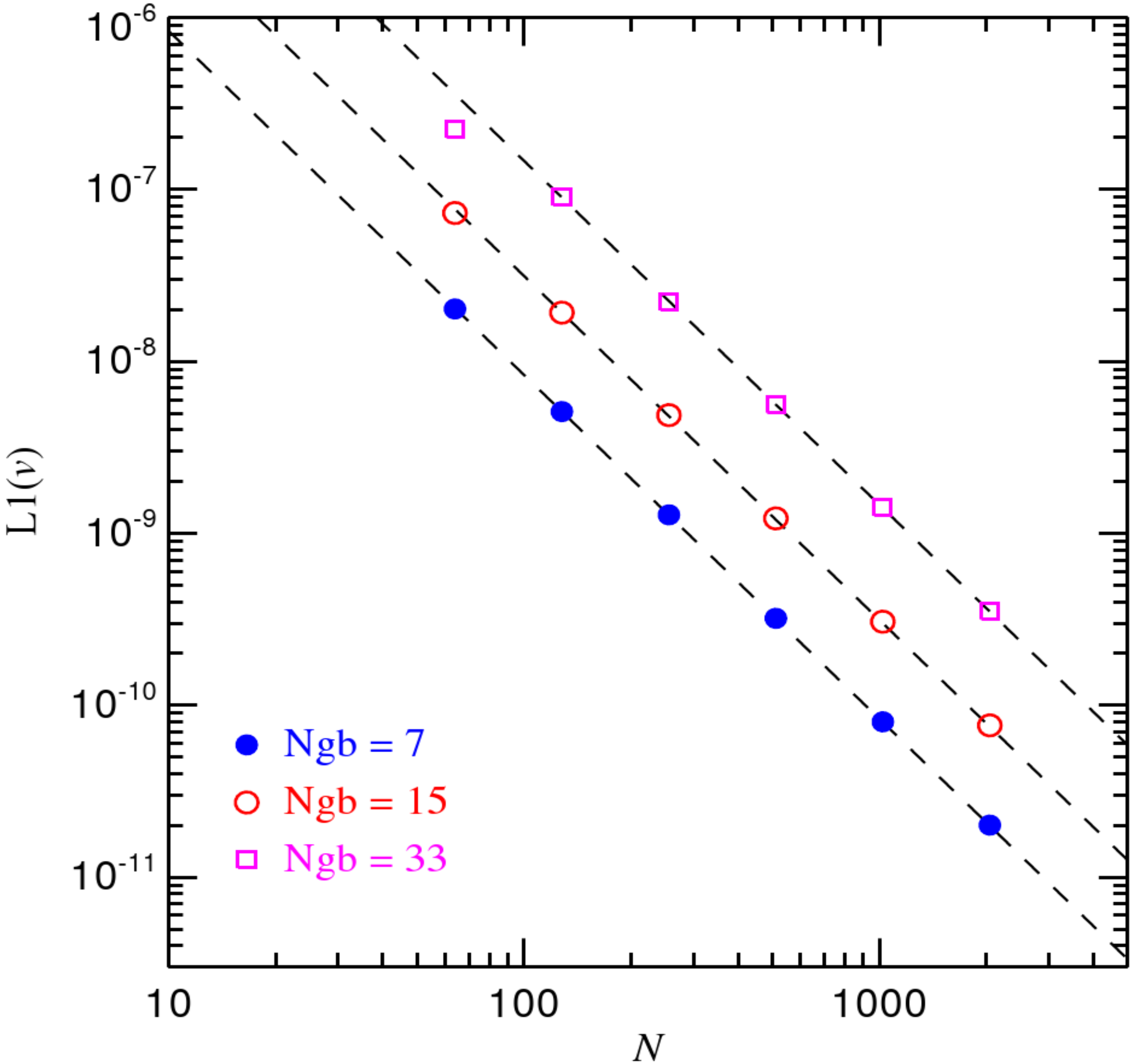

$L1 \sim N^{-2}$

A couple of basic shock tubes calculated with the GADGET SPH code

TWO SHOCK PROBLEMS AND A STRONG RAREFACTION

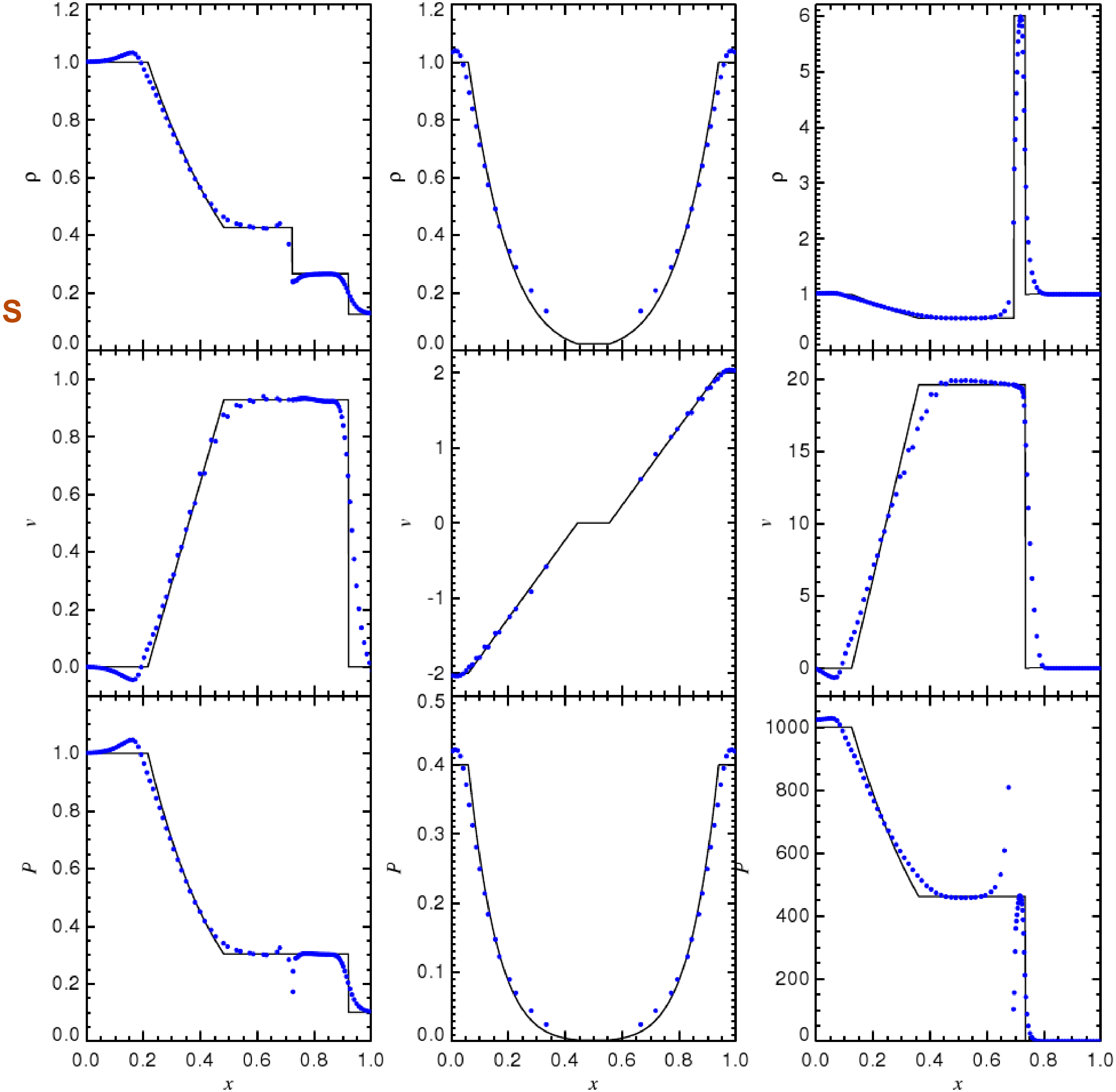

SPH convergence rate for basic Riemann problems

ERROR NORM FOR THE VELOCITY AS A FUNCTION OF RESOLUTION

$L1 \sim N^{-1}$

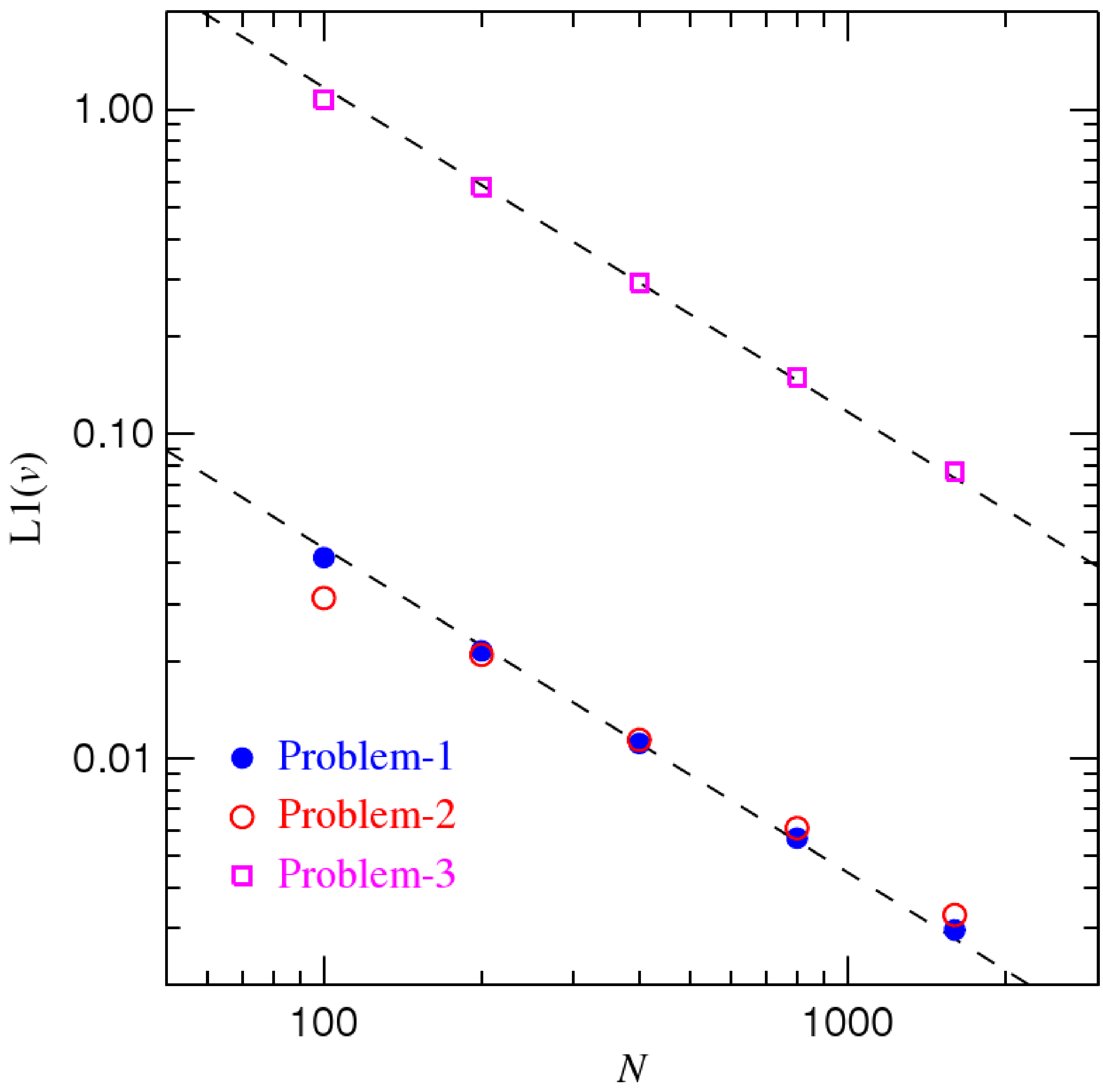

SPH shock tube problem and its convergence **in 2D**

PARTICLE VELOCITIES, AND ERROR NORM AS A FUNCTION OF RESOLUTION

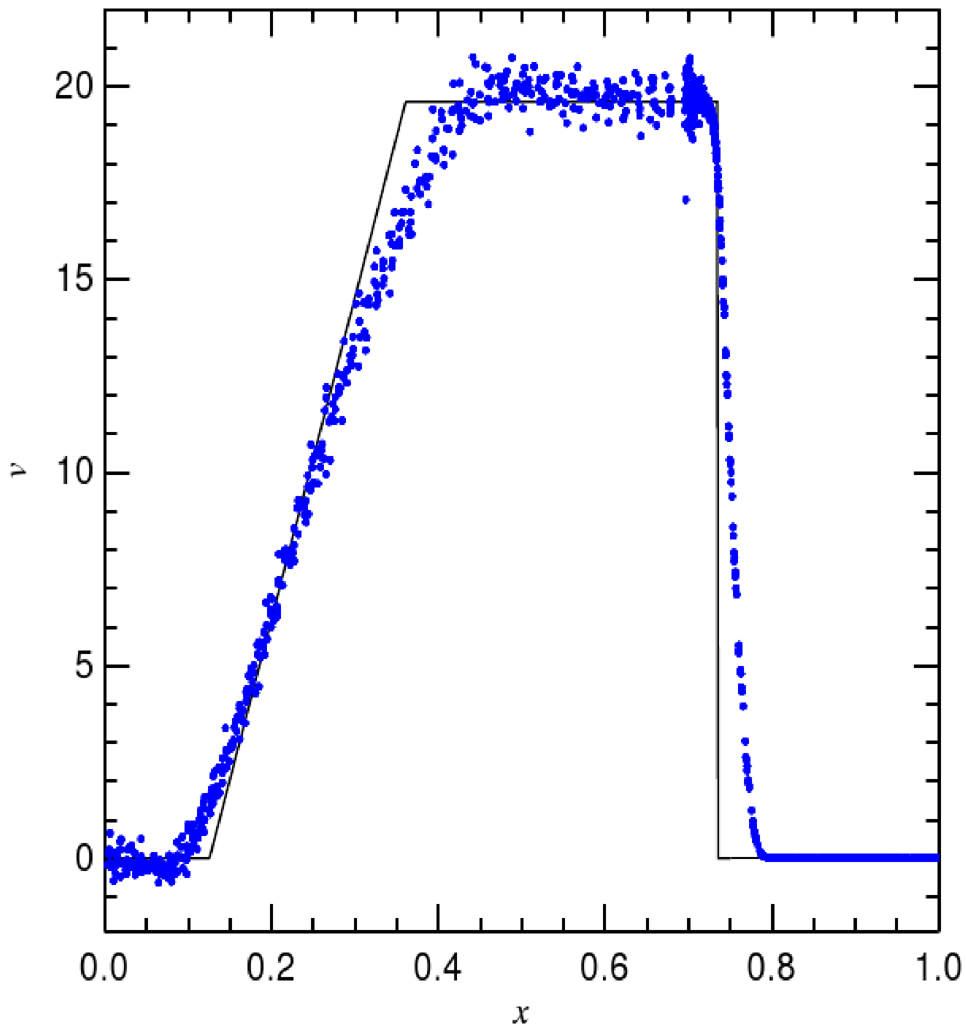

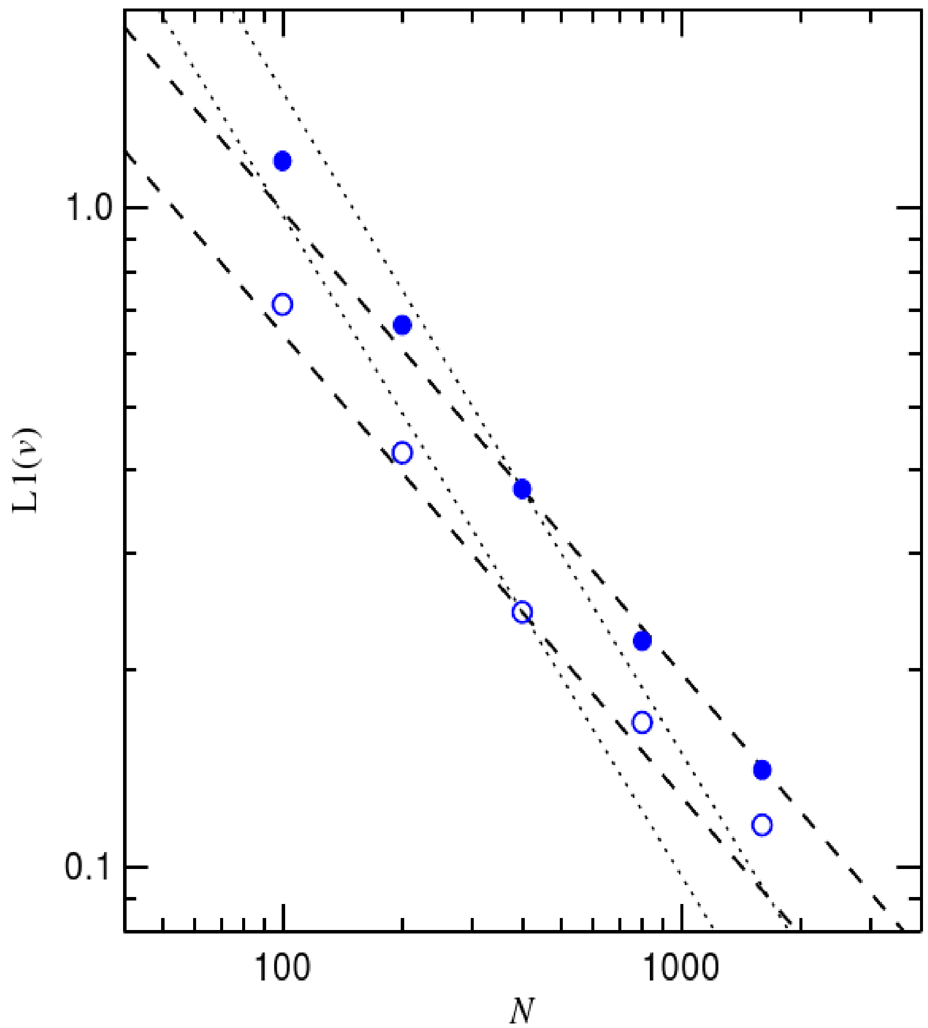

L1 ~ $N^{-0.7}$

Open circles: binned result
filled circles: particles directly

The Gresho vortex test in two dimensions

EVOLUTION OF A STATIONARY VORTEX FLOW

Initial conditions:

$$v_\phi(r) = \begin{cases} 5r & \text{for} \quad 0 \le r < 0.2 \\ 2 - 5r & \text{for} \quad 0.2 \le r < 0.4 \\ 0 & \text{for} \quad r \ge 0.4 \end{cases}$$

$$P(r) = \begin{cases} 5 + 25/2r^2 & \text{for} \quad 0 \le r < 0.2 \\ 9 + 25/2r^2 - \\ \quad 20r + 4\ln(r/0.2) & \text{for} \quad 0.2 \le r < 0.4 \\ 3 + 4\ln 2 & \text{for} \quad r \ge 0.4 \end{cases}$$

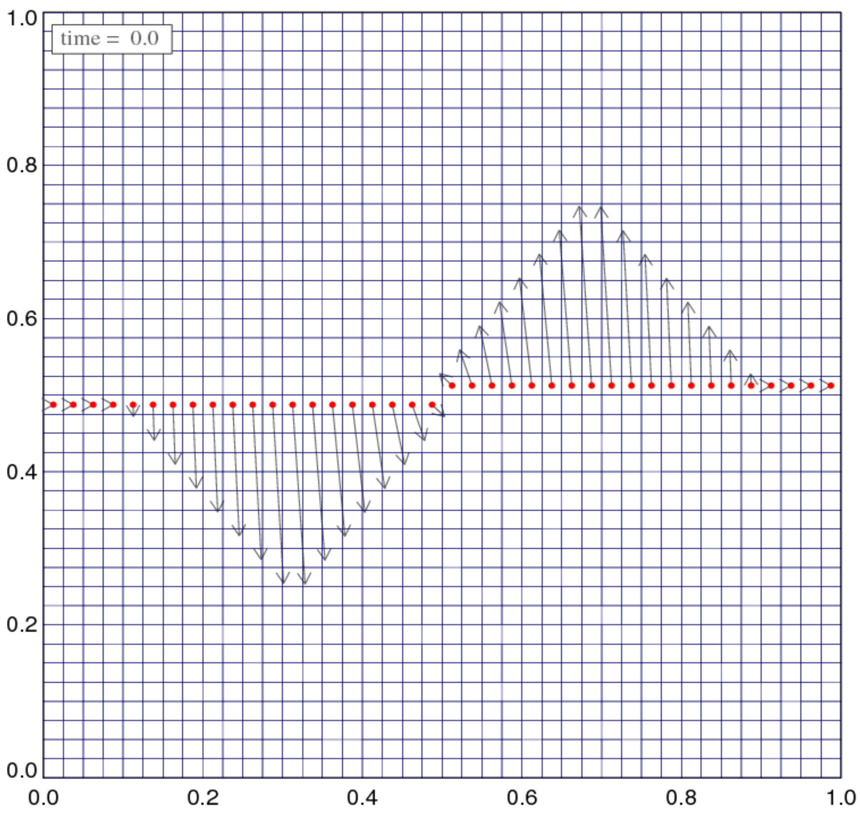

The Gresho vortex test done with SPH

AZIMUTHAL VELOCITY PROFILE AT T=1.0 FOR A 80 x 80 INITIAL GRID

standard SPH

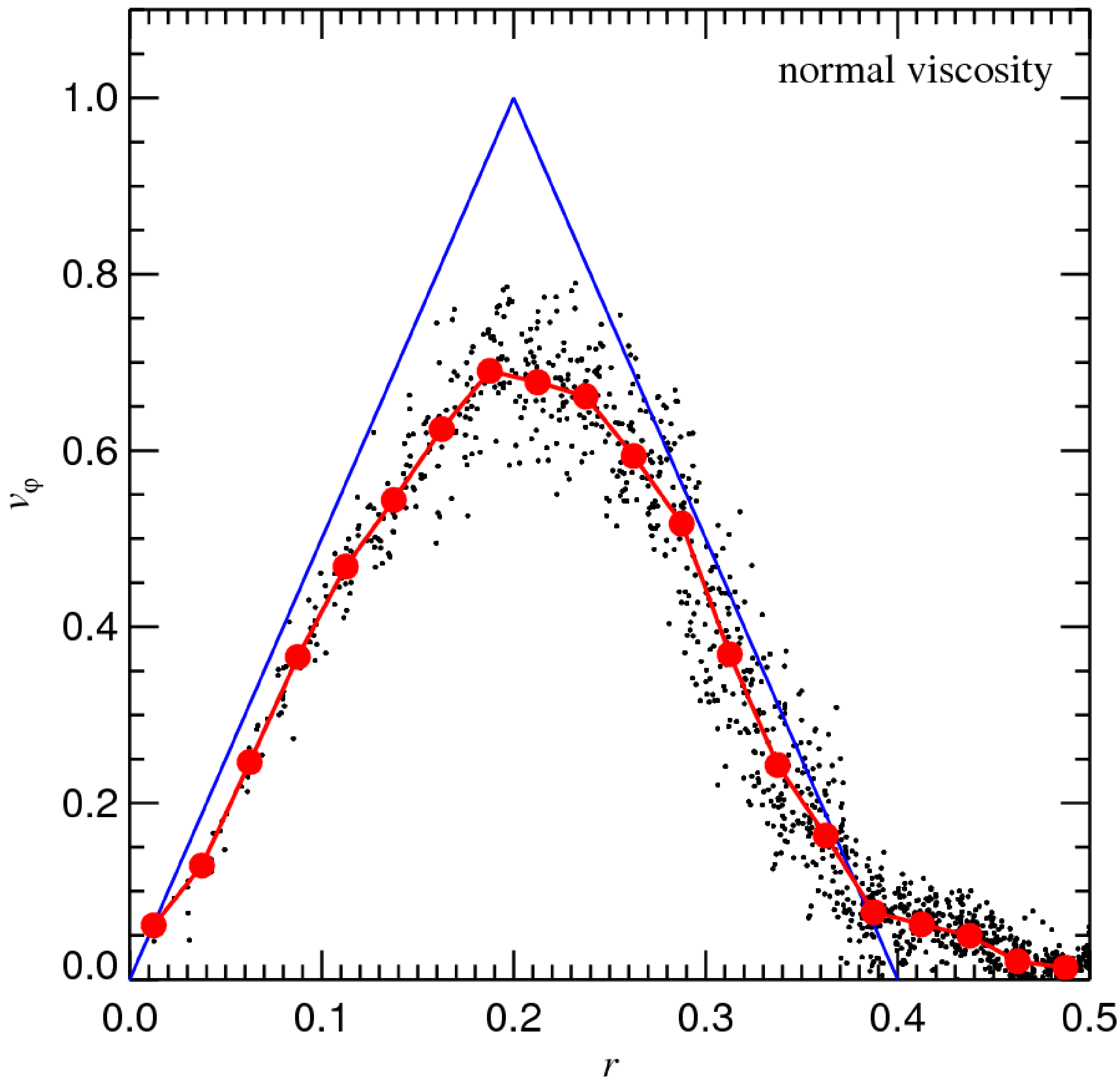

The Gresho vortex test done with SPH

AZIMUTHAL VELOCITY PROFILE AT T=1.0 FOR A 80 x 80 INITIAL GRID

reduced viscosity

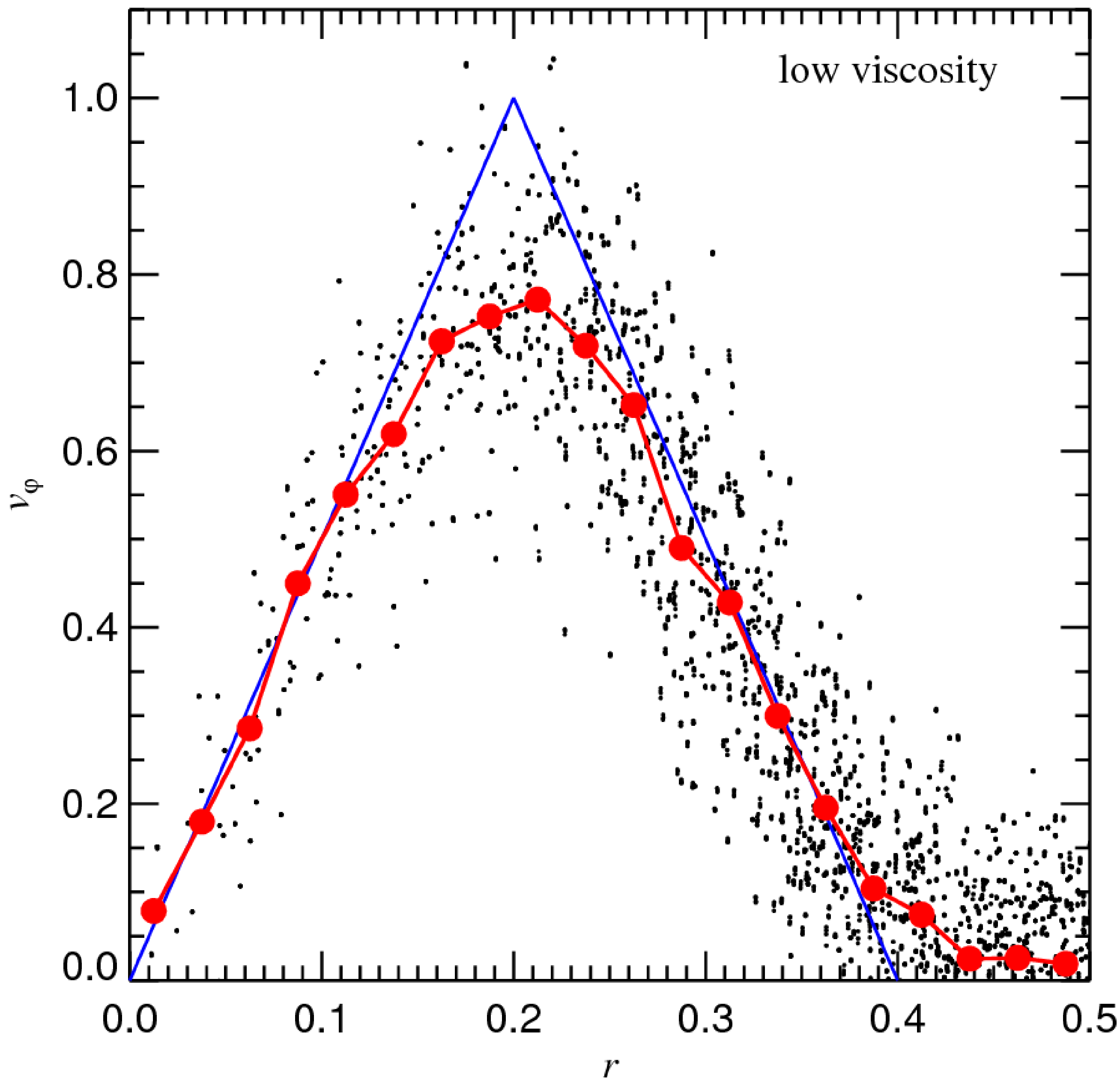

The Gresho vortex test done with SPH

AZIMUTHAL VELOCITY PROFILE AT T=1.0 FOR A 80 x 80 INITIAL GRID

no viscosity

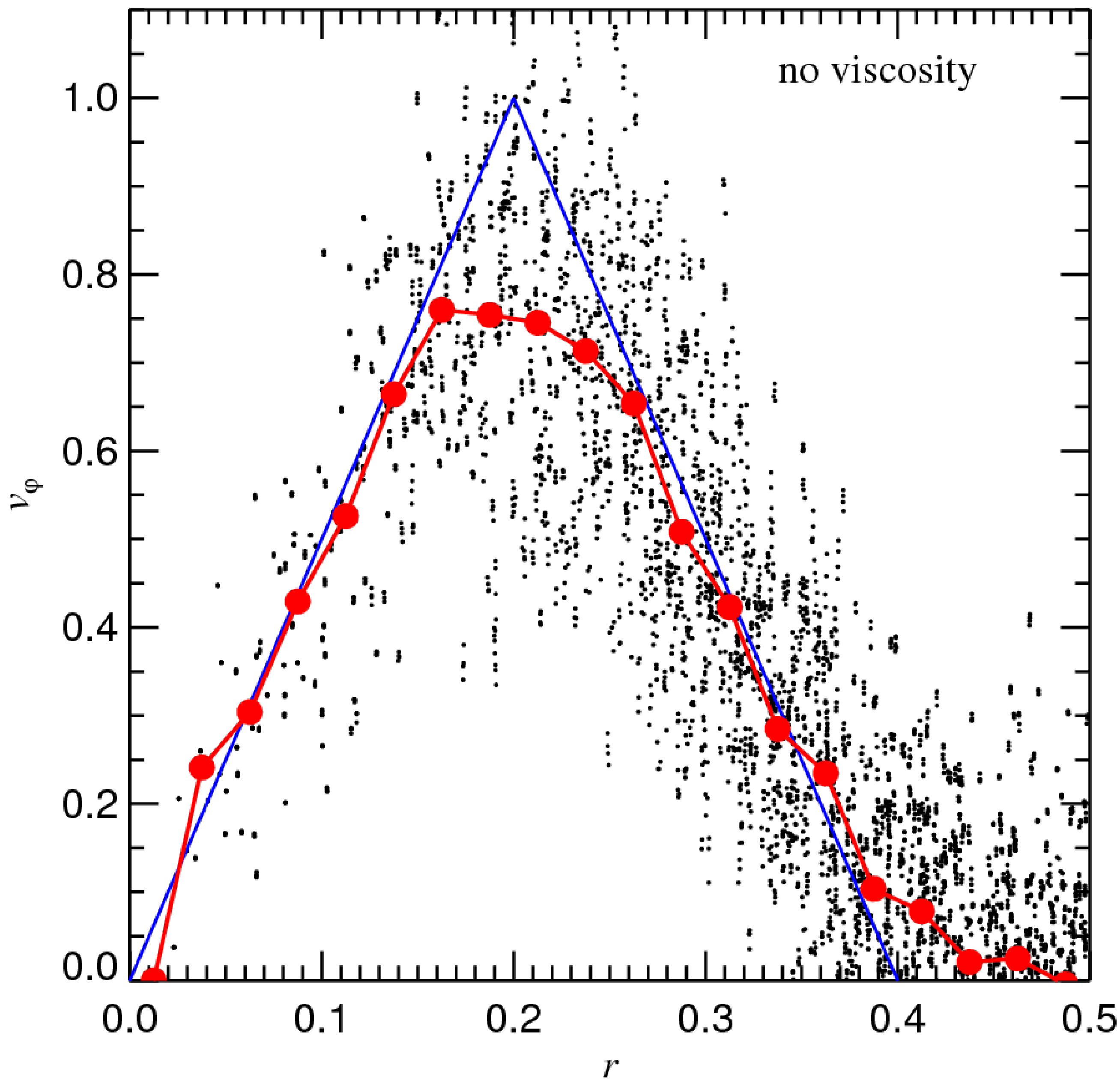

The Gresho vortex test done with SPH

CONVERGENCE RATE AGAINST ANALYTIC/HIGHEST-RES SOLUTION

dashed line:
$L1 \sim N^{-0.7}$

Note, for AREPO:
$L1 \sim N^{-1.4}$

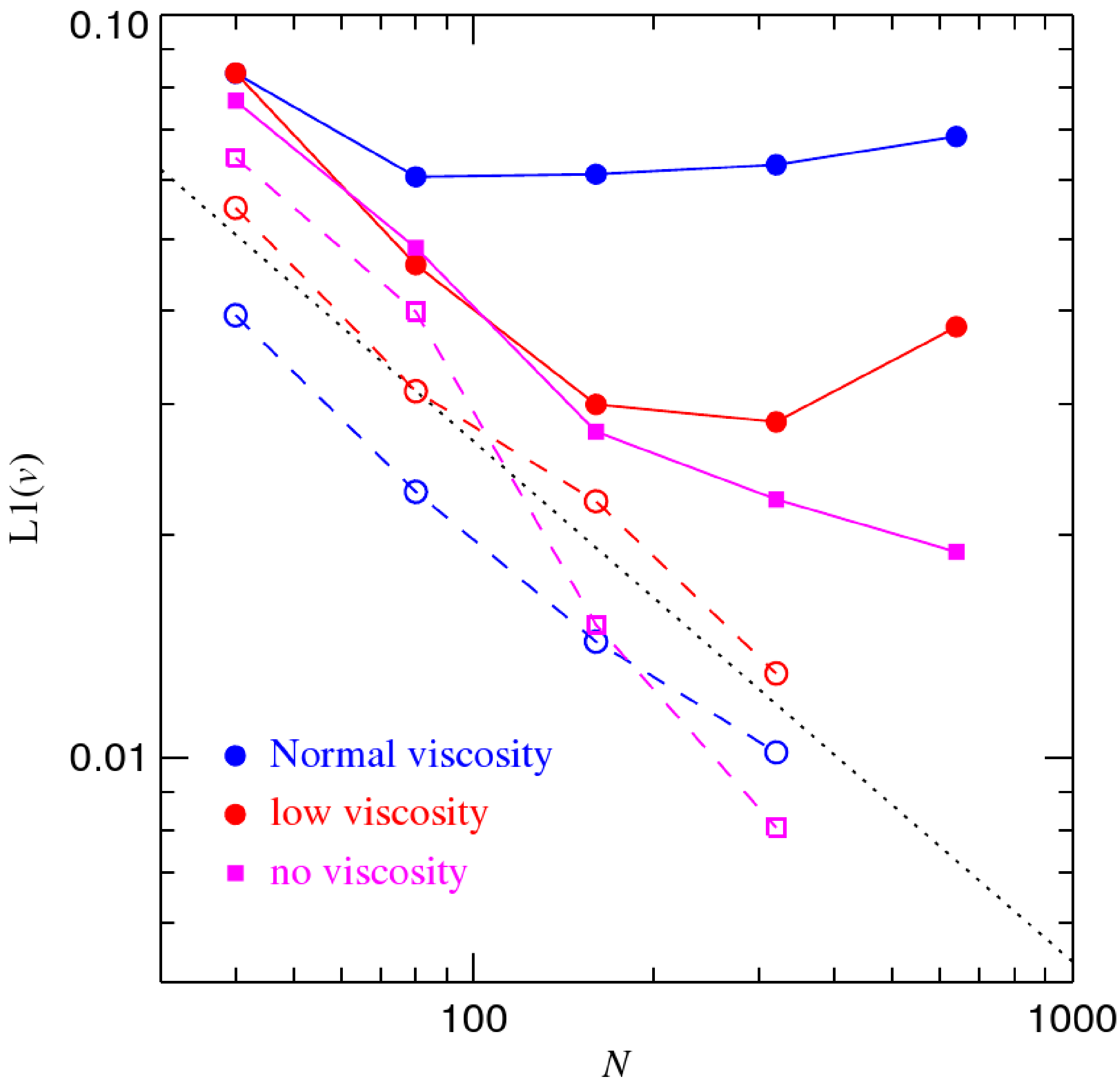

Fluid instabilities and mixing in SPH

A cloud moving through ambient gas shows markedly different long-term behavior in SPH and Eulerian mesh codes

DISRUPTION OF A CLOUD BY KELVIN-HELMHOLTZ INSTABILITIES

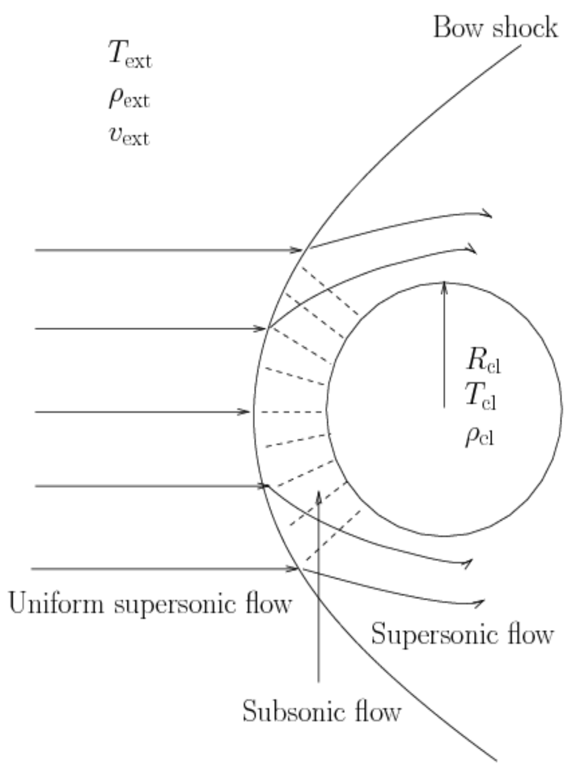

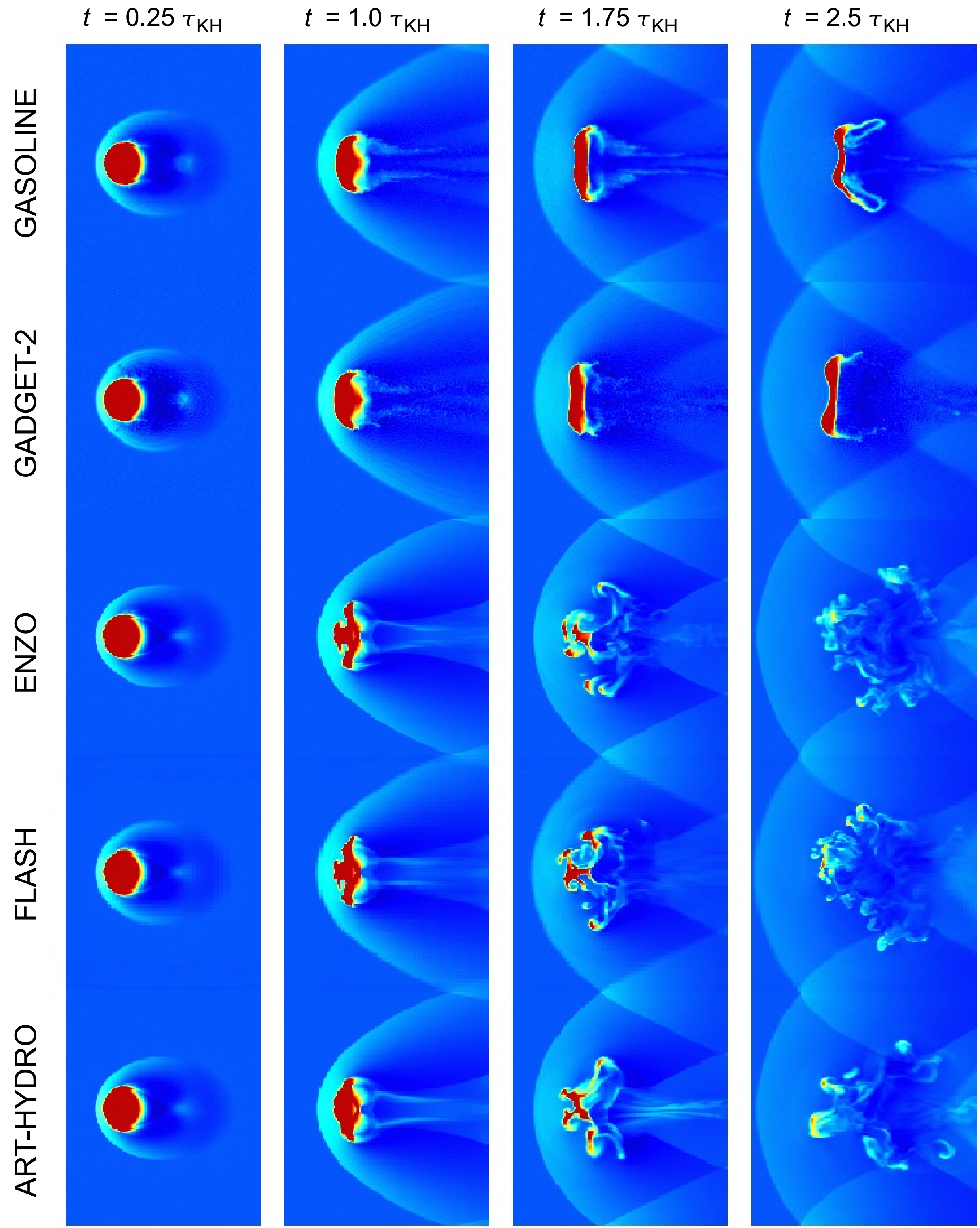

Agertz et al. (2007)

In SPH, fluid instabilities at contact discontinuities with large density jumps tend to be suppressed by a spurious numerical surface tension

KELVIN-HELMHOLTZ INSTABILITIES IN SPH

Agertz et al. (2007)

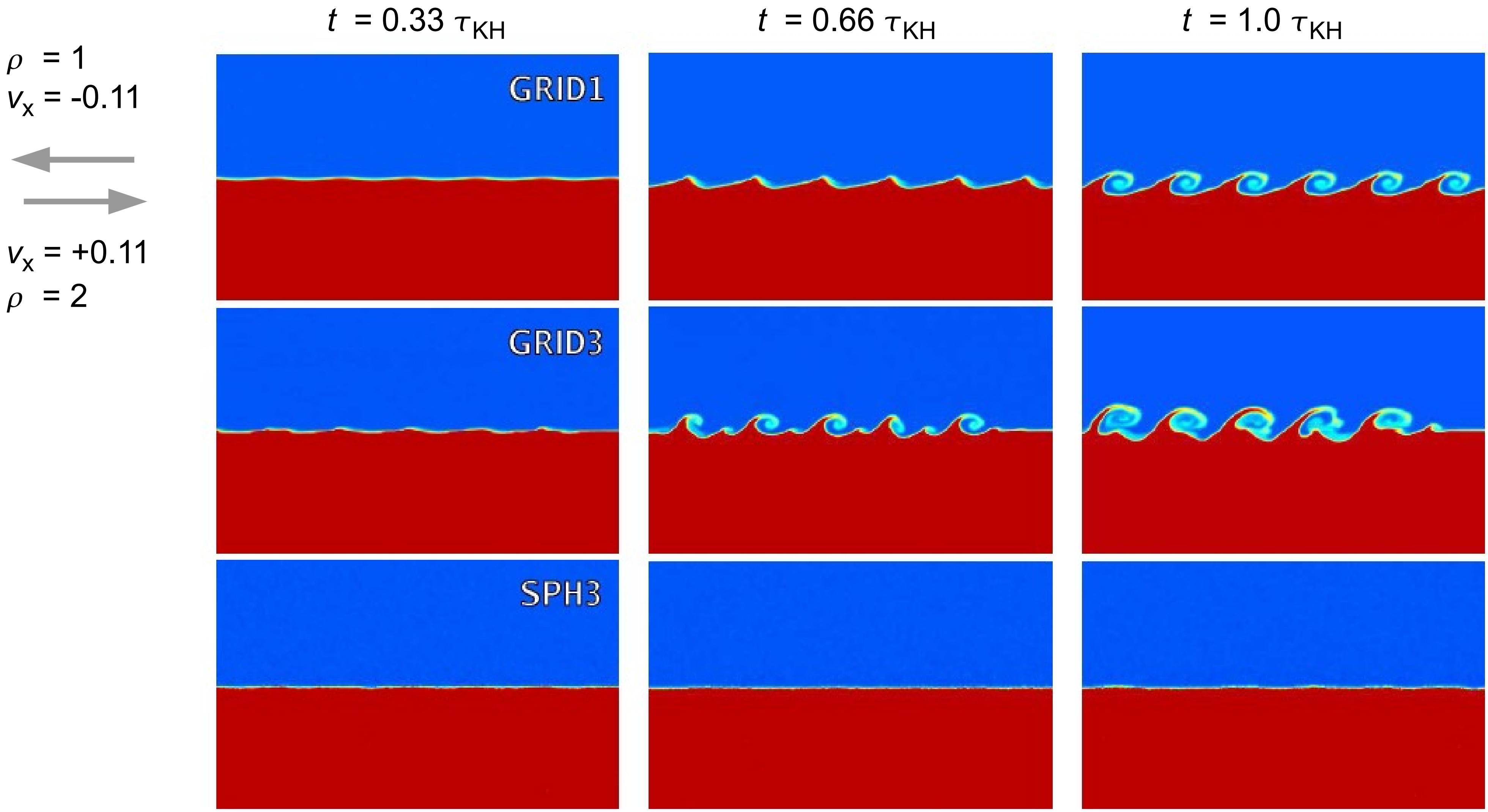

Thought experiment on mixing

A simple *Gedankenexperiment* about mixing in SPH

$\rho_1 = 8$

$u_1 = \frac{1}{8}$

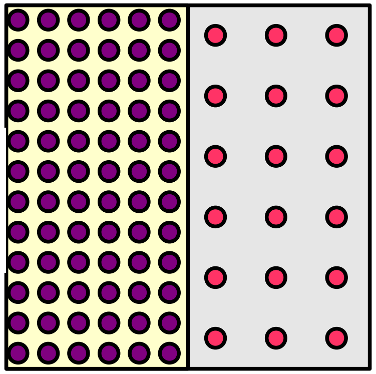

$V_1 = \frac{1}{2}$ $V_2 = \frac{1}{2}$

$\rho_2 = 1$

$u_2 = 1$

The pressure is constant:

$$P_1 = (\gamma - 1)\rho_1 u_1 = \frac{2}{3} \qquad P_2 = P_1$$

The specific entropies are:

$$A_i = \frac{P_i}{\rho_i^\gamma} \qquad A_1 = \frac{1}{48} \qquad A_2 = \frac{2}{3}$$

Let's calculate the total thermal energy of the system:

$$E_{\rm therm} = \int \frac{A\rho^{\gamma-1}}{\gamma - 1}\,{\rm d}m$$

$$E_{\rm therm} = 1$$

We now mix the particles, keeping their specific entropies fixed:

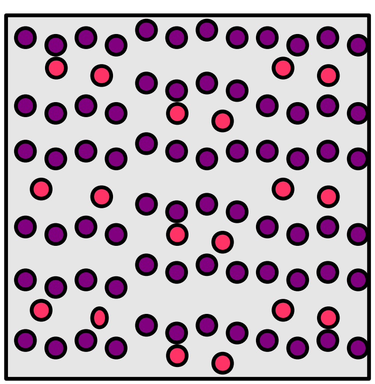

All particles estimate the same mean density: $M_{\rm tot} = \frac{9}{2} \qquad \overline{\rho} = \frac{9}{2}$

The thermal energy thus becomes:

$$E_{\rm therm} = \frac{M_1 A_1 \overline{\rho}^{2/3}}{2/3} + \frac{M_2 A_2 \overline{\rho}^{2/3}}{2/3}$$

$$E_{\rm therm} = \frac{5}{8}\left(\frac{9}{2}\right)^{2/3} \simeq 1.7$$

➡ **This mixing process is energetically forbidden!**

What happened to the entropy in our *Gedankenexperiment* ?

In slowly mixing the two phases, we preserve the total thermal energy:

Expect: $\overline{u} = \frac{2}{9}$ $\quad\quad$ $\overline{A} = \frac{2}{3}\frac{\overline{u}}{\overline{\rho}^{2/3}}$ $\quad\quad$ $\overline{A} = \frac{2^{8/3}}{3^{13/3}} \simeq 0.054$

The Sackur-Tetrode equation for the entropy of an ideal gas can be written as:

$$S = \frac{3}{2}\frac{k_{\rm B}}{\mu} M \left[\ln\left(\frac{P}{\rho^{\gamma}}\right) + \ln\left(\frac{2\pi\mu^{8/3}}{h^2}\right) + \frac{5}{3} \right]$$

If the mass in a system is conserved, it is sufficient to consider the simplified entropy:

$$\tilde{S} = M \ln A$$

When the system is mixed, the change of the entropy is:

$$\Delta\tilde{S} = M_{\rm tot} \ln \overline{A} - (M_1 \ln A_1 + M_2 \ln A_2)$$

$$\Delta\tilde{S} \simeq 2.55 \quad \geq \quad 0$$

→ **Unless this entropy is generated somehow, SPH will have problems to mix different phases of a flow.**

(Aside: Mesh codes can generate entropy outside of shocks – this allows them to treat mixing.)

New developments in SPH that try to address mixing

Artificial heat conduction at contact discontinuities has been proposed as a solution for the suppressed fluid instabilities

ARTIFICIAL HEAT MIXING TERMS

Price (2008) **Wadsley, Veeravalli & Couchman (2008)**

Price argues that in SPH every conservation law requires dissipative terms to capture discontinuities.

The normal artificial viscosity applies to the momentum equation, but discontinuities in the (thermal) energy equation should also be treated with a dissipative term.

For every conserved quantity *A*

$$\sum_j m_j \mathrm{d}A_j/\mathrm{d}t = 0$$

a dissipative term is postulated

$$\left(\frac{\mathrm{d}A_i}{\mathrm{d}t}\right)_{\mathrm{diss}} = \sum_j m_j \frac{\alpha_A v_{\mathrm{sig}}}{\bar{\rho}_{ij}} (A_i - A_j) \hat{\mathbf{r}}_{ij} \cdot \nabla W_{ij}$$

that is designed to capture discontinuities.

This is the discretized form of a diffusion problem:

$$\left(\frac{\mathrm{d}A}{\mathrm{d}t}\right)_{\mathrm{diss}} \approx \eta \nabla^2 A$$

$$\eta \propto \alpha v_{\mathrm{sig}} |r_{ij}|$$

Artificial heat conduction drastically improves SPH's ability to account for fluid instabilities and mixing

COMPARISON OF KH TESTS FOR DIFFERENT TREATMENTS OF THE DISSIPATIVE TERMS

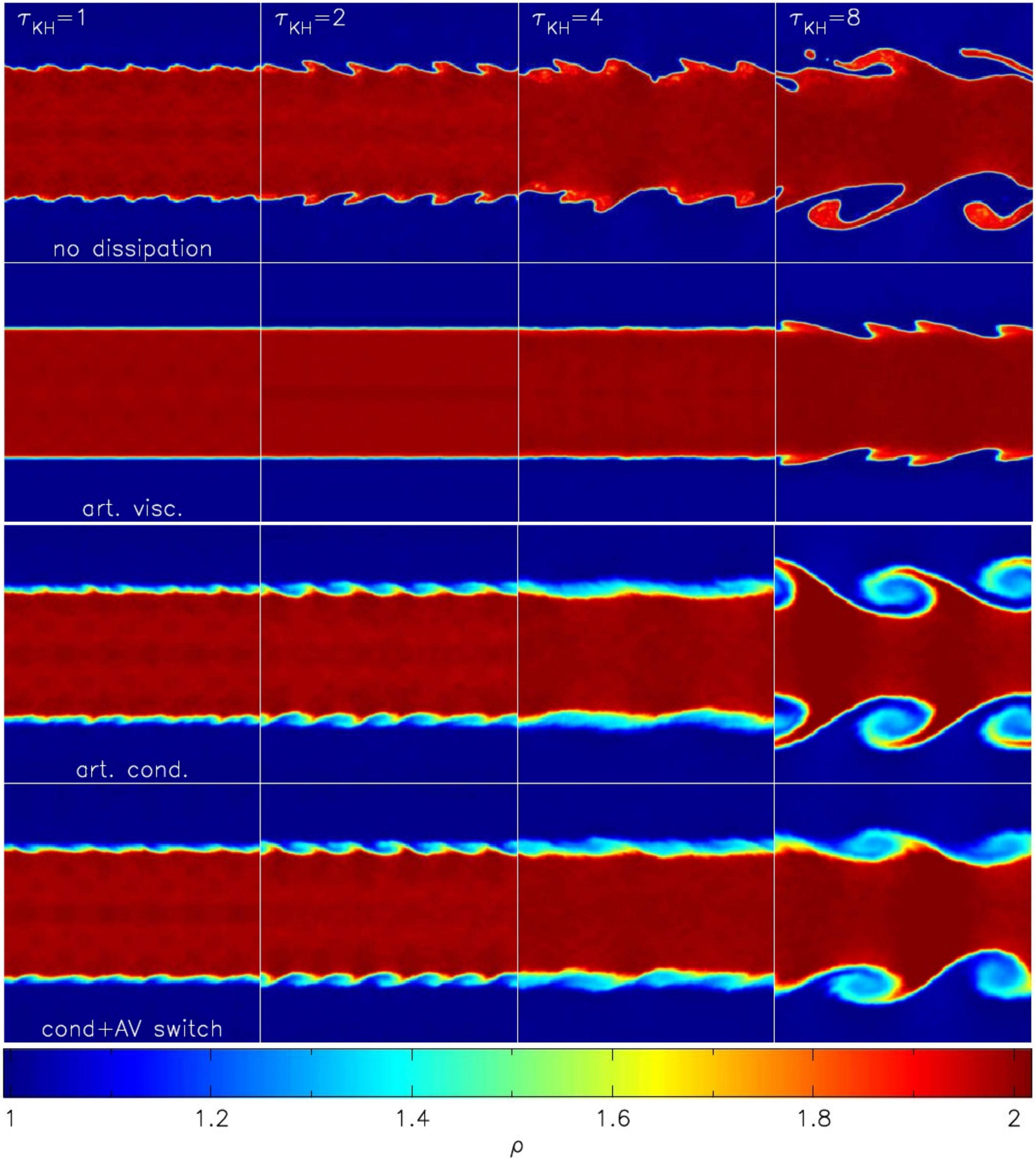

Price (2008)

Another route to better SPH may lie in different ways to estimate the density

AN ALTERNATIVE SPH FORMULATION

"Mixing SPH" of **Read, Hayfield, Agertz (2009)**

- Density estimate like Ritchie & Thomas (2001):

$$\rho_i = \sum_j^N \left(\frac{A_j}{A_i}\right)^{\frac{1}{\gamma}} m_j \overline{W}_{ij}$$

- Very large number of neighbors (442 !) to beat down noise
- Needs peaked kernel to suppress clumping instability
- This in turn reduces the order of the density estimate, so that a large number of neigbors is required.

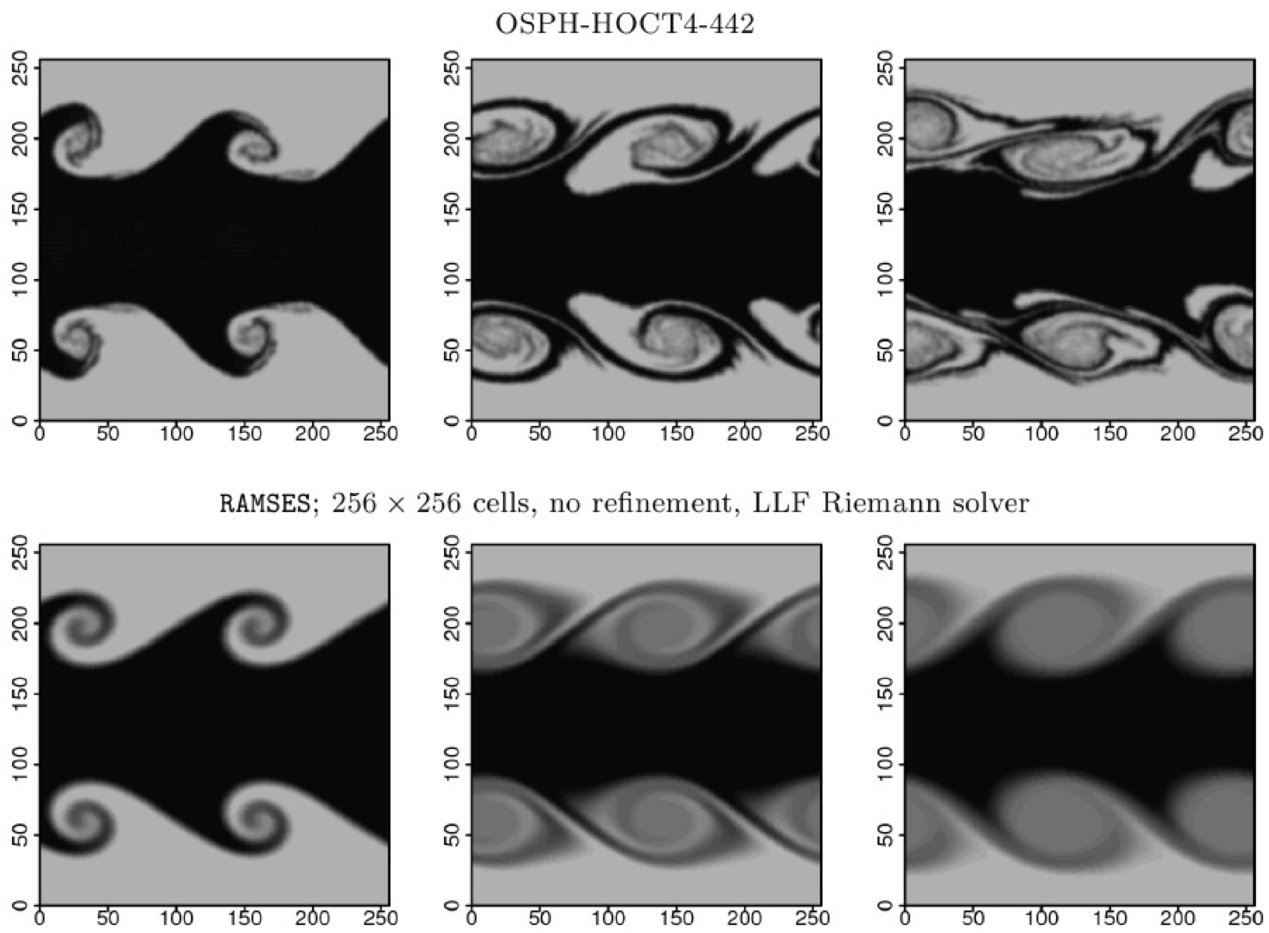

Alternative formulations

Voronoi and Delaunay tessellations provide unique partitions of space based on a given sample of mesh-generating points

BASIC PROPERTIES OF VORONOI AND DELAUNAY MESHES

Voronoi mesh

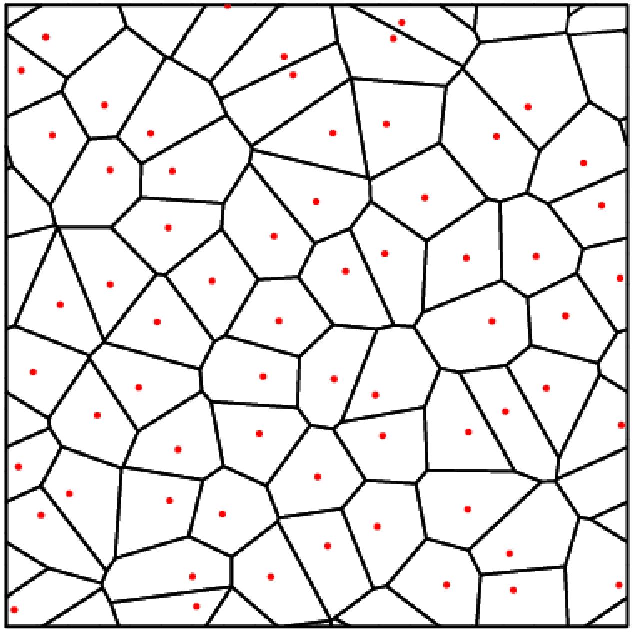

Delaunay triangulation

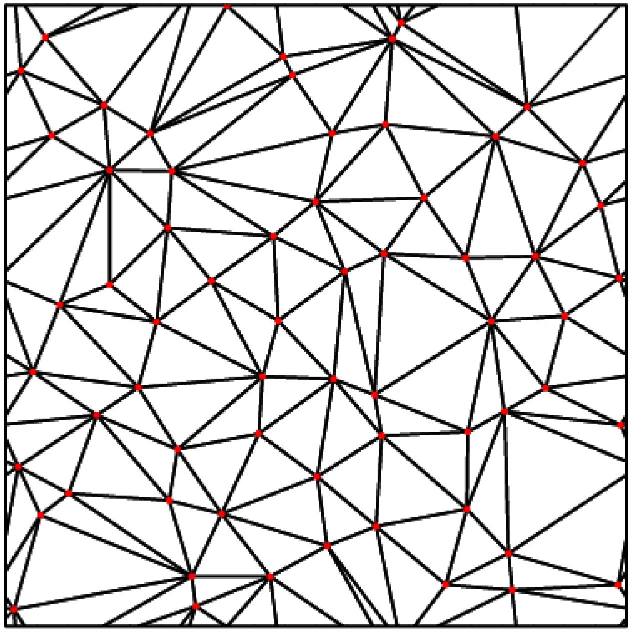

both shown together

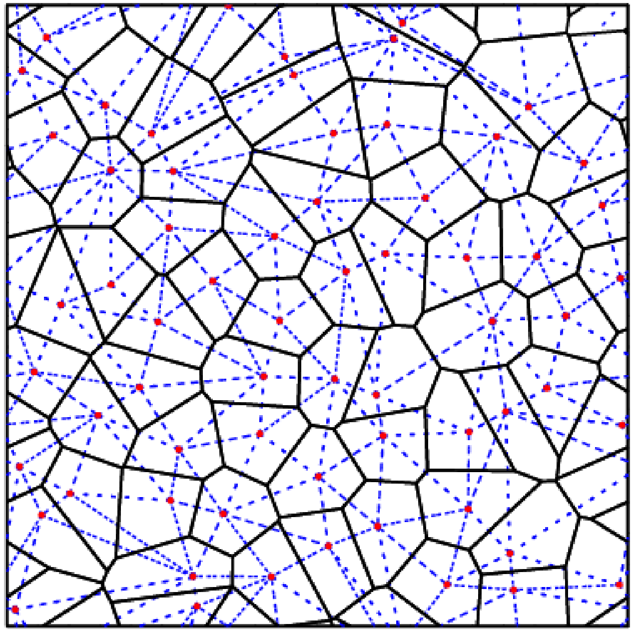

Each Voronoi cell contains the **space closest** to its generating point

The Delaunay triangulation contains only triangles with an **empty circumcircle**. The Delaunay tiangulation maximizes the minimum angle occurring among all triangles.

The centres of the circumcircles of the Delaunay triangles are the vertices of the Voronoi mesh. In fact, the two tessellations are the topological **dual graph** to each other.

Voronoi particle hydrodynamics replaces SPH's density estimate

DERIVATION OF VPH EQUATIONS OF MOTION

Hess & Springel (2010)

Discretized Fluid Lagrangian:

$$L = \sum_i \left[\frac{1}{2} m_i \, \boldsymbol{v}_i^2 - m_i \, u_i(\rho_i, s_i) \right]$$

Voronoi Density Estimate:

$$\rho_i = \frac{m_i}{V_i}$$

Equations of motion:

$$m_i \ddot{\boldsymbol{r}}_i = \sum_{j \neq i} A_{ij} (P_i - P_j) \left(\frac{\boldsymbol{c}_{ij}}{R_{ij}} + \frac{\boldsymbol{e}_{ij}}{2} \right)$$

equivalent form:

$$m_i \ddot{\boldsymbol{r}}_i = -\sum_{j \neq i} A_{ij} \left[(P_i + P_j) \frac{\boldsymbol{e}_{ij}}{2} + (P_j - P_i) \frac{\boldsymbol{c}_{ij}}{R_{ij}} \right]$$

VPH shows no surface tension at strong contact discontinuities

EVOLUTION OF AN OVERDENSE ELLIPSIOIDAL BLOB IN SPH AND VPH

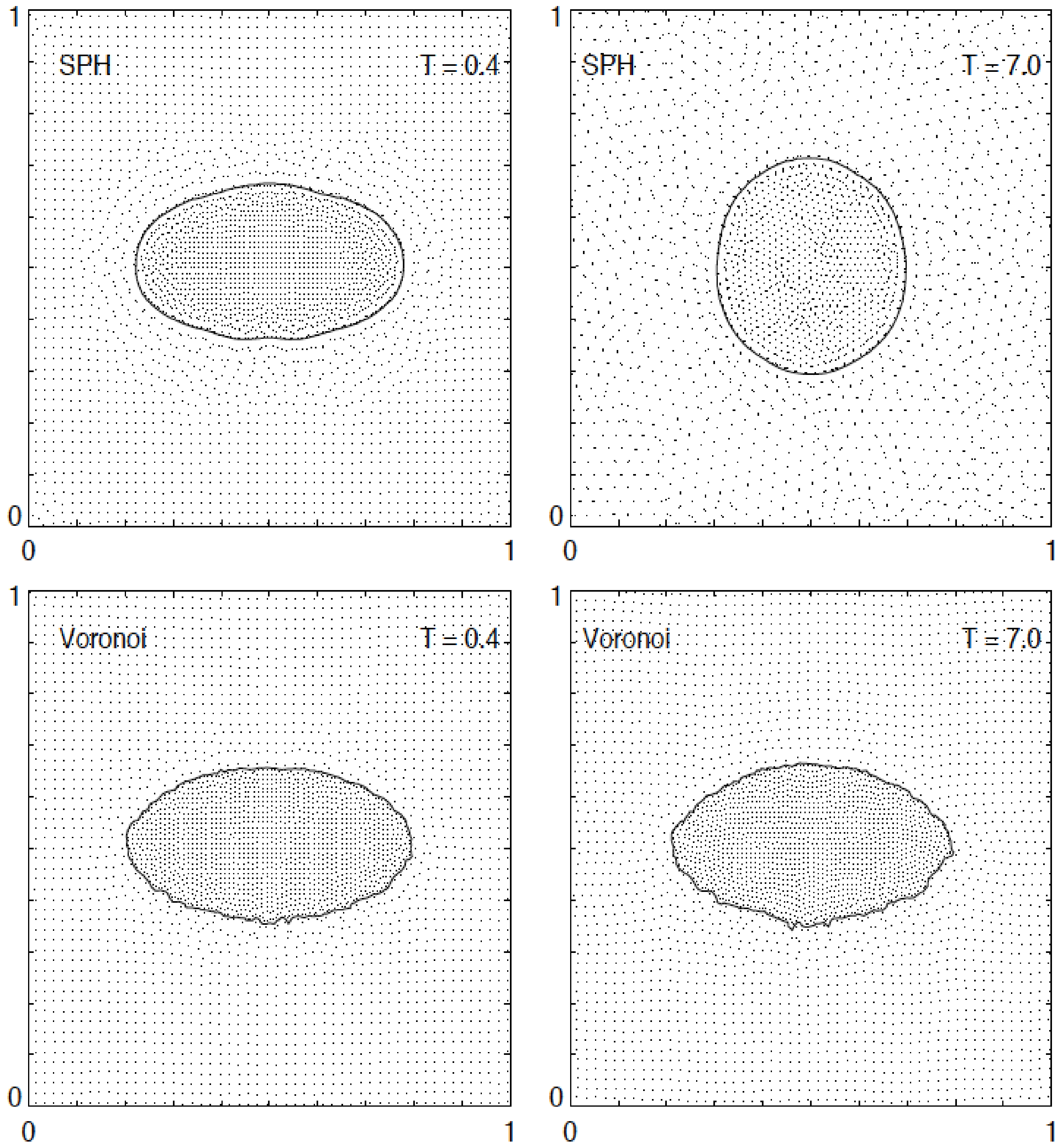

Overall, the accuracy of VPH is however quite similar to SPH, but the code complexity is considerably larger

Moving-mesh hydrodynamics with AREPO

Volker Springel

Heidelberg Institute for Theoretical Studies

HITS

Universität Heidelberg

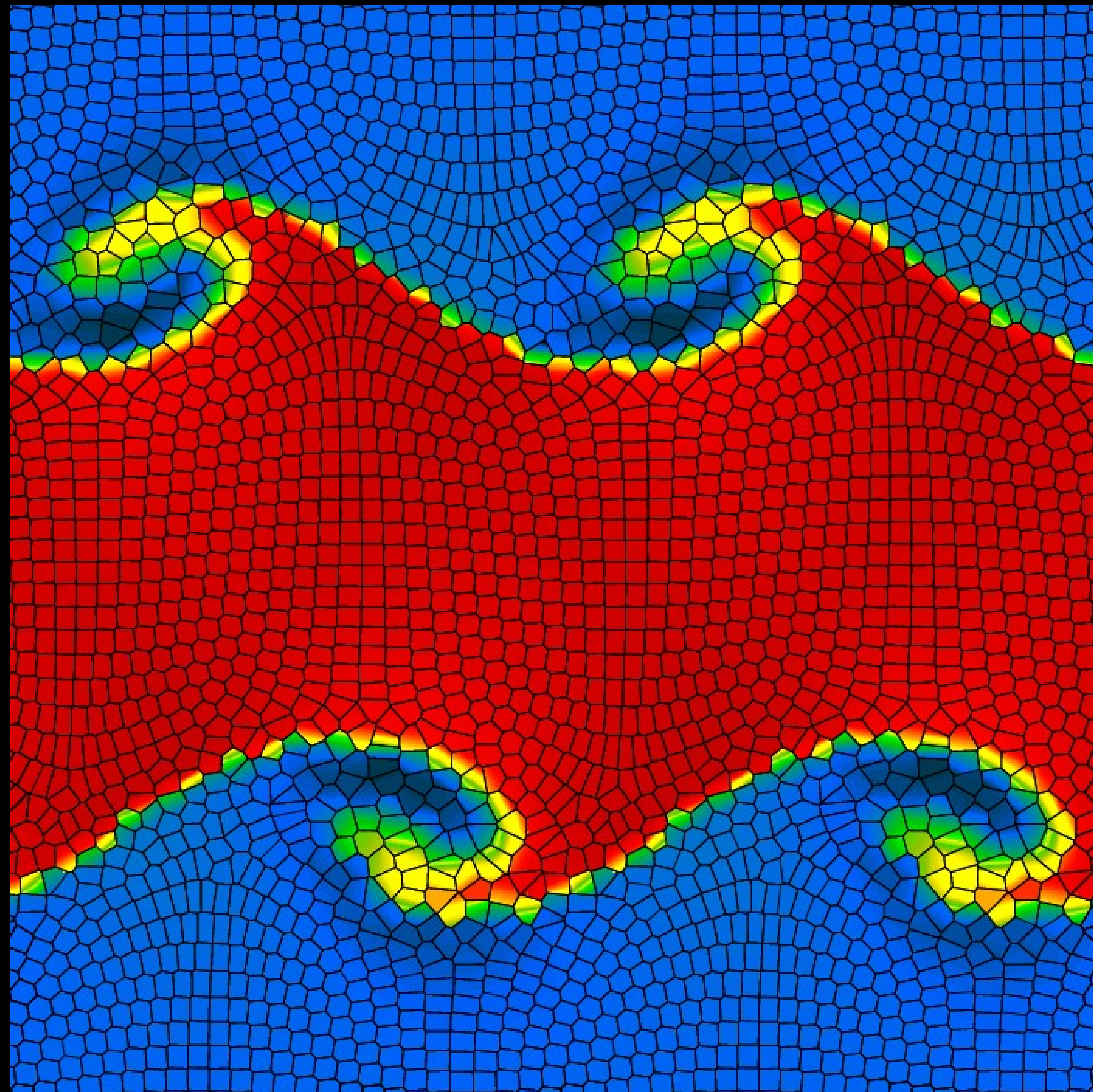

A finite volume discretization of the Euler equations on a moving mesh can be readily defined

THE EULER EQUATIONS AS HYPERBOLIC SYSTEM OF CONSERVATION LAWS

Euler equations

$$\frac{\partial \mathbf{U}}{\partial t} + \nabla \cdot \mathbf{F} = 0$$

State vector

$$\mathbf{U} = \begin{pmatrix} \rho \\ \rho \mathbf{v} \\ \rho e \end{pmatrix}$$

Flux vector

$$\mathbf{F}(\mathbf{U}) = \begin{pmatrix} \rho \mathbf{v} \\ \rho \mathbf{v}\mathbf{v}^T + P \\ (\rho e + P)\mathbf{v} \end{pmatrix}$$

$$e = u + \mathbf{v}^2/2$$

Equation of state: $P = (\gamma - 1)\rho u$

Discretization in terms of a number of finite volume cells:

Cell averages

$$\mathbf{Q}_i = \begin{pmatrix} M_i \\ \mathbf{p}_i \\ E_i \end{pmatrix} = \int_{V_i} \mathbf{U}\, \mathrm{d}V$$

Evolution equation

$$\frac{\mathrm{d}\mathbf{Q}_i}{\mathrm{d}t} = -\int_{\partial V_i} \left[\mathbf{F}(\mathbf{U}) - \mathbf{U}\mathbf{w}^T\right] \mathrm{d}\mathbf{n}$$

But how to compute the fluxes through cell surfaces?

The fluxes are calculated with an exact Riemann solver in the frame of the moving cell boundary

SKETCH OF THE FLUX CALCULATION

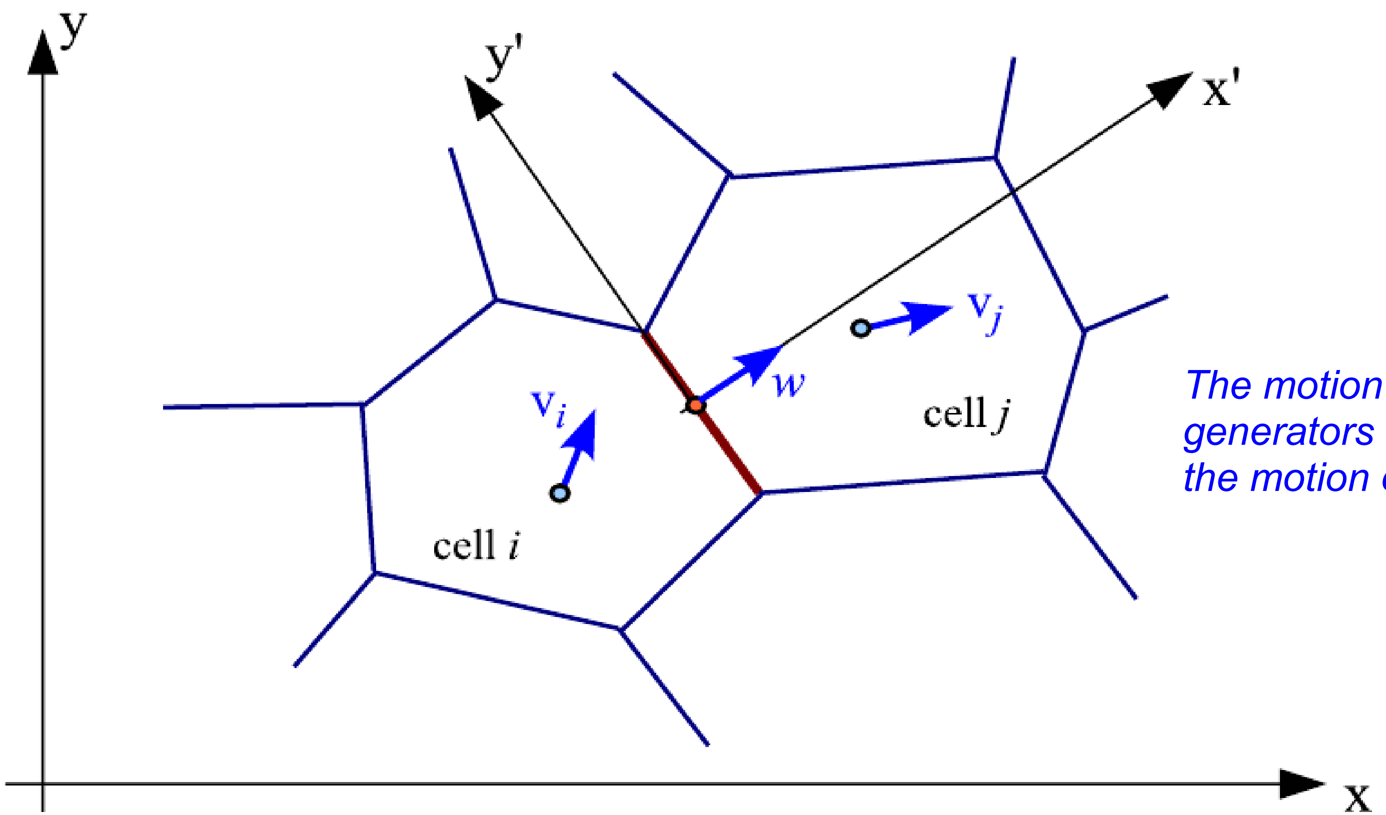

The motion of the mesh generators uniquely determines the motion of all cell boundaries

State left of cell face **State right of cell face**

$$\begin{pmatrix} \rho_L \\ \mathbf{v}_L \\ P_L \end{pmatrix} \quad \begin{pmatrix} \rho_R \\ \mathbf{v}_R \\ P_R \end{pmatrix} \longrightarrow \text{Riemann solver (in frame of cell face)} \longrightarrow \begin{pmatrix} \rho \\ \mathbf{v} \\ P \end{pmatrix} \longrightarrow \mathbf{F}(\mathbf{U})$$

Riemann solver
(in frame of cell face)

A differentially rotating gaseous disk with strong shear can be simulated well with the moving mesh code

MODEL FOR A CENTRIFUGALLY SUPPORTED, THIN DISK

$$\Sigma(r) = \Sigma_0 \exp(-r/h)$$

$$v_c^2(r) \equiv r\frac{\partial \Phi}{\partial r} = 2\frac{Gm}{h}y^2\left[I_0(y)K_0(y) - I_1(y)K_1(y)\right]$$

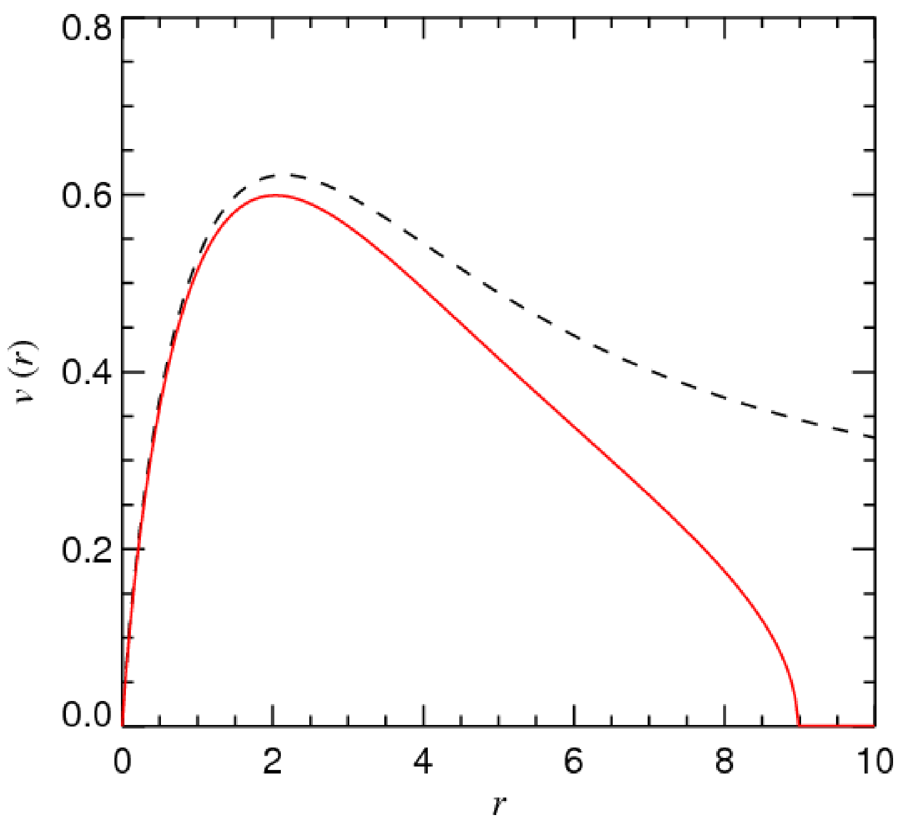

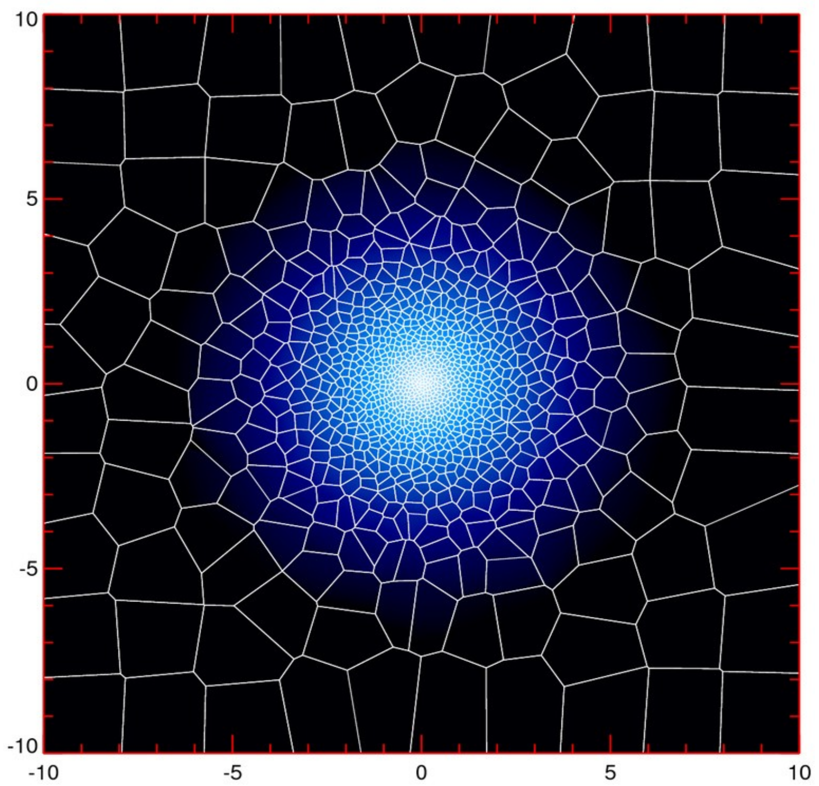

Different examples of test problems with the moving-mesh code

Sedov-Taylor Exposion

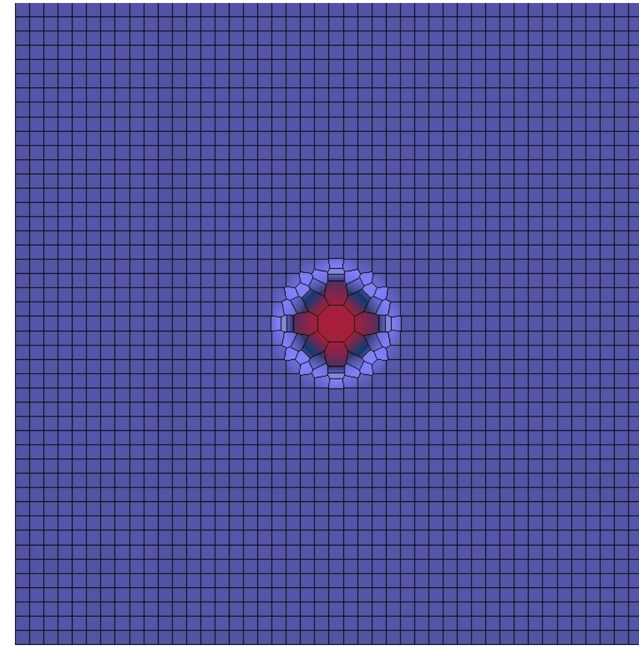

High-resolution
Kelvin-Helmholtz instability

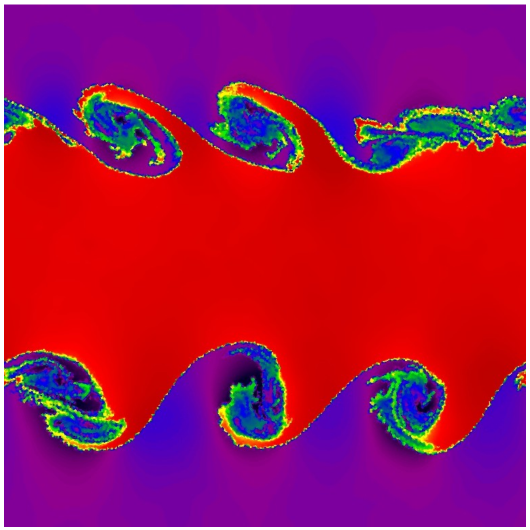

Rayleigh-Taylor (with visible mesh)

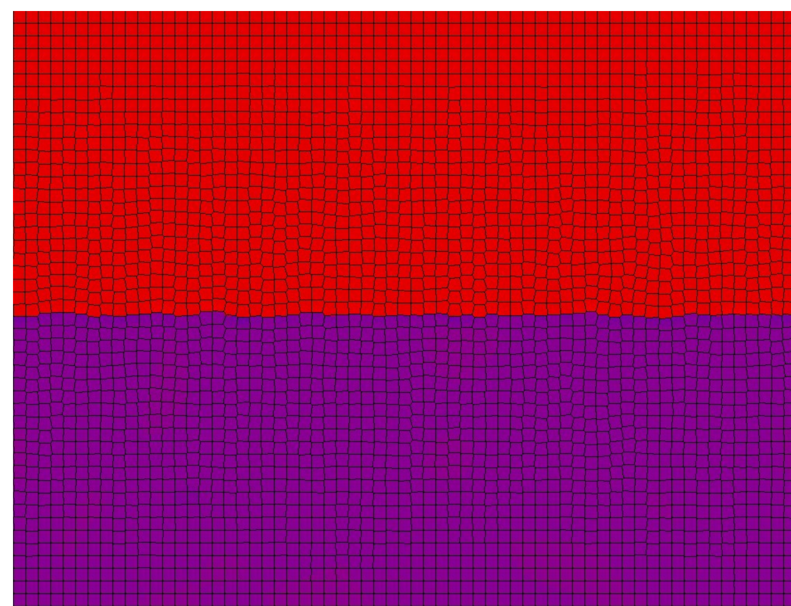

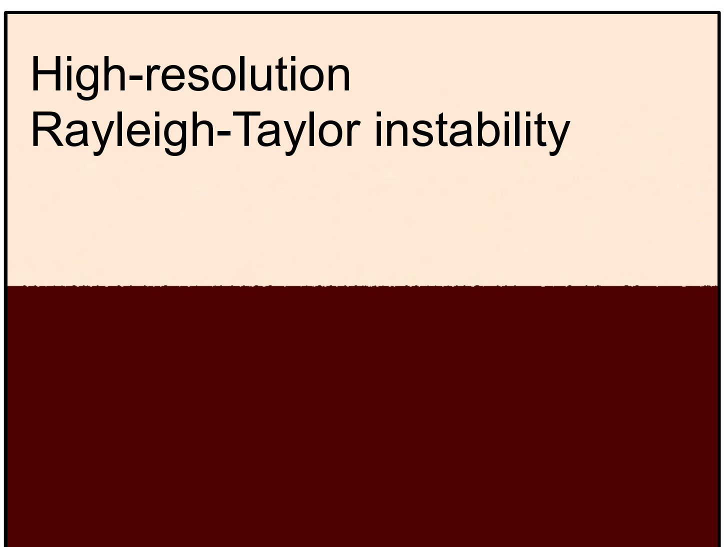

Interacting double blast-problem of Woodward & Colella

MOVING AND FIXED MESH SOLUTIONS WITH EQUAL NUMBER OF RESOLUTIN ELEMENTS

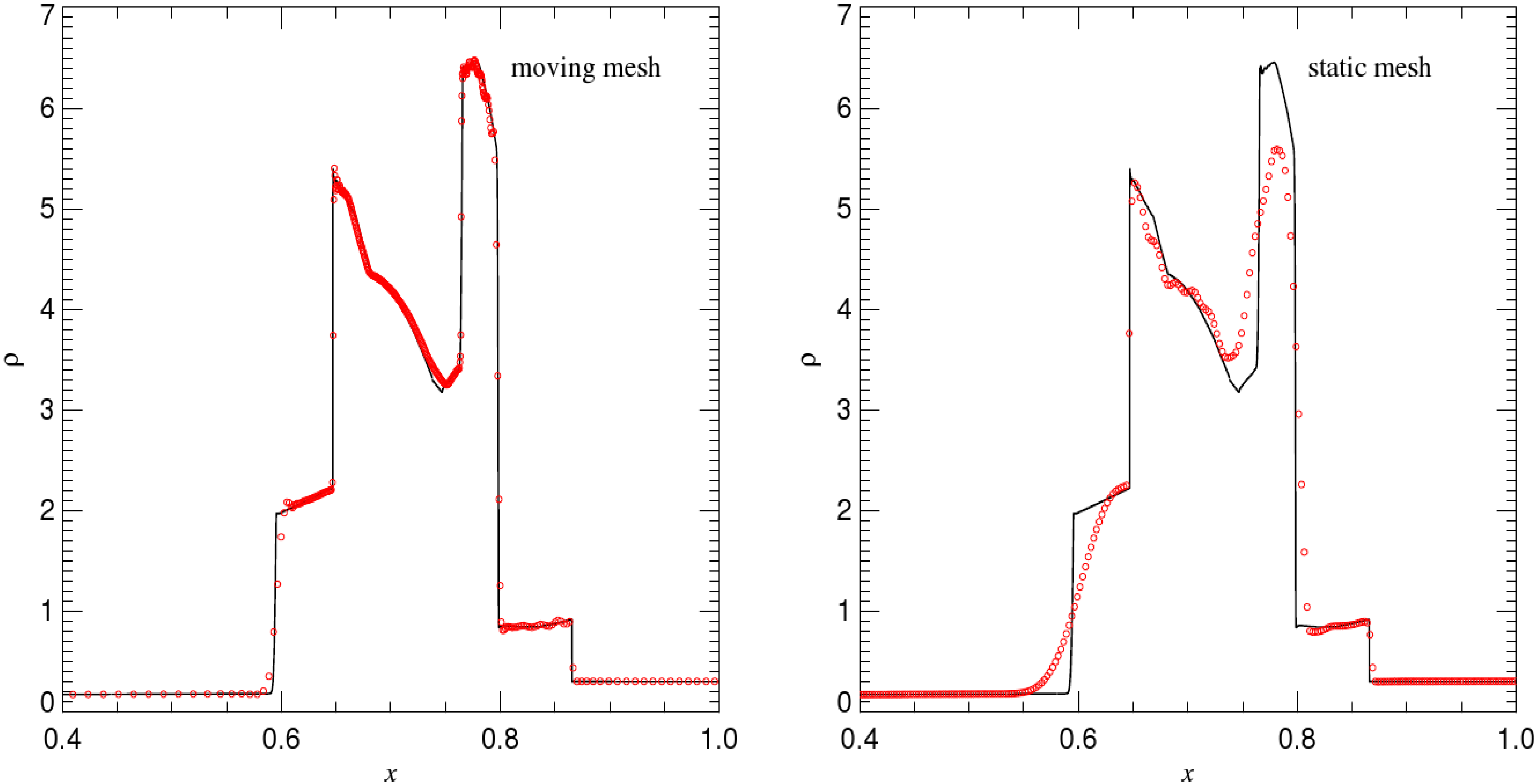

The Gresho vortex test in two dimensions

EVOLVED AZIMUTHAL VELOCITY PROFILE FOR DIFFERENT CODES AND BOOSTS

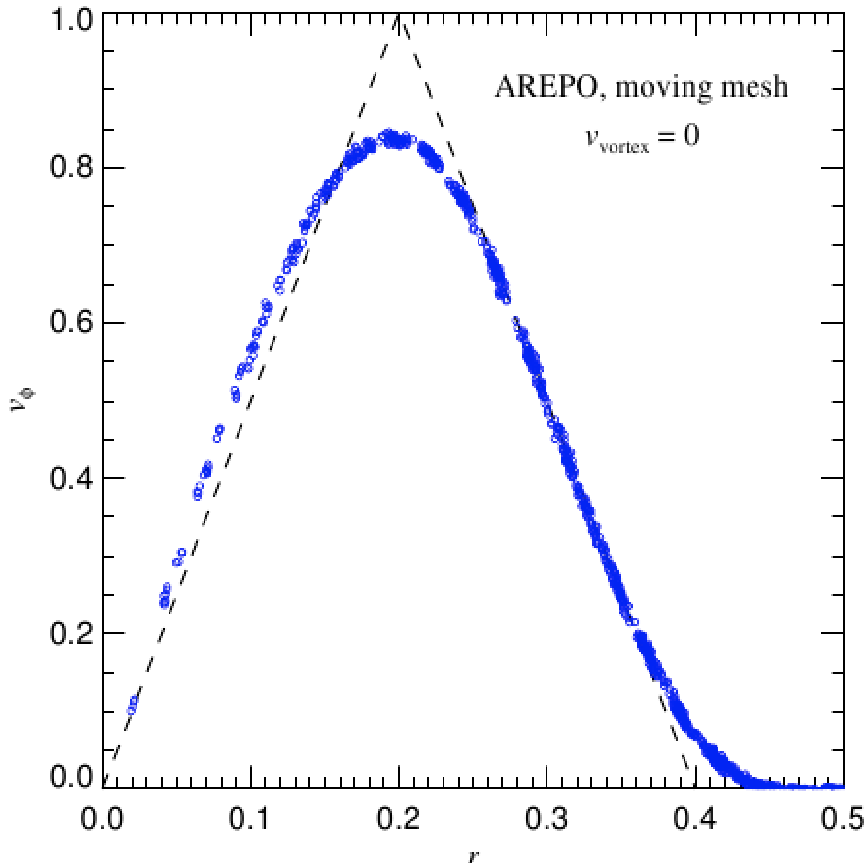

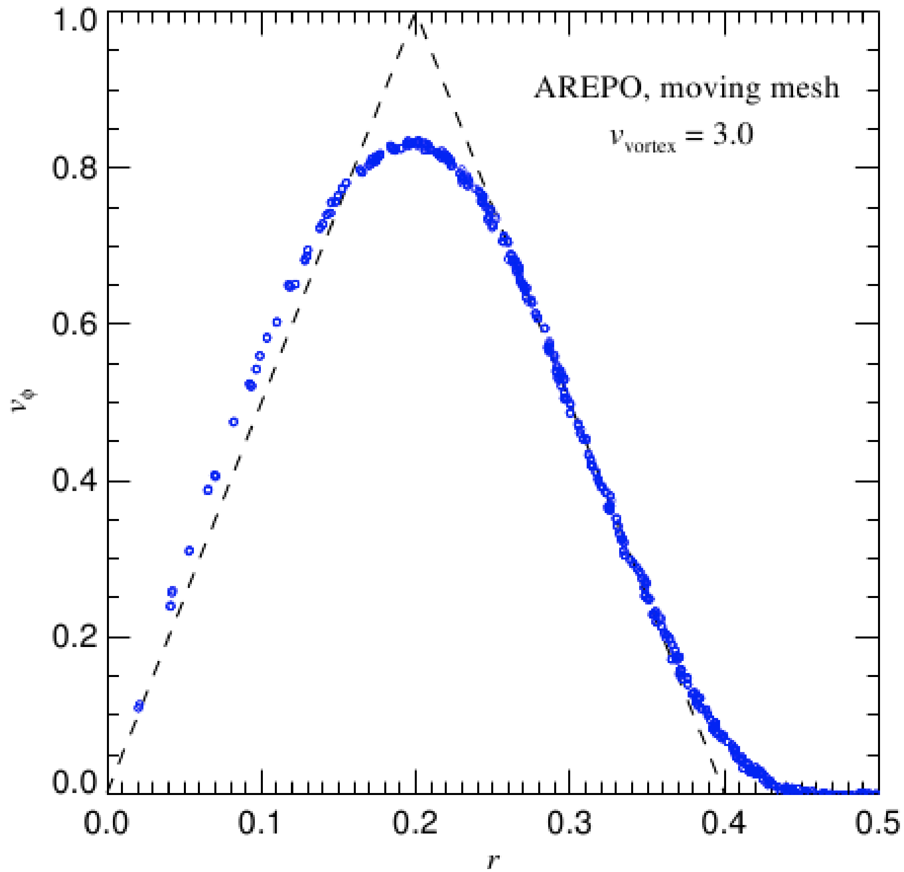

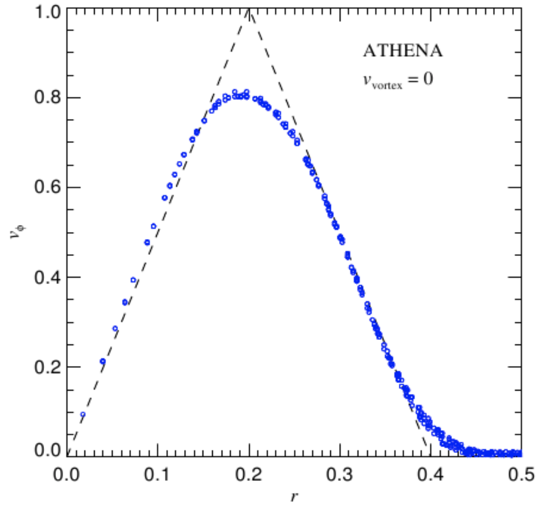

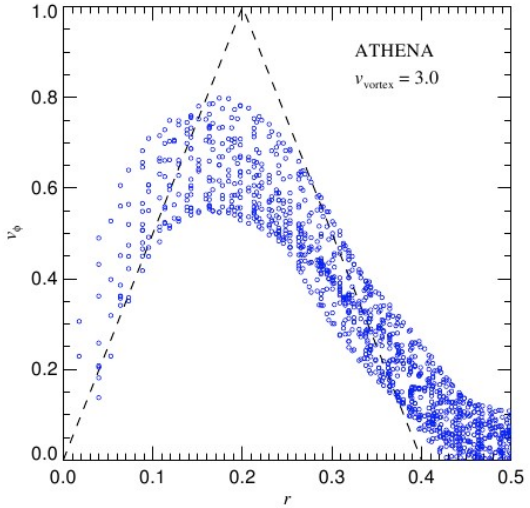

The Gresho vortex test in two dimensions

CONVERGENCE RATE AGAINST ANALYTIC SOLUTION FOR AREPO AND ATHENA

Solid line:
L1 ~ $N^{-1.4}$

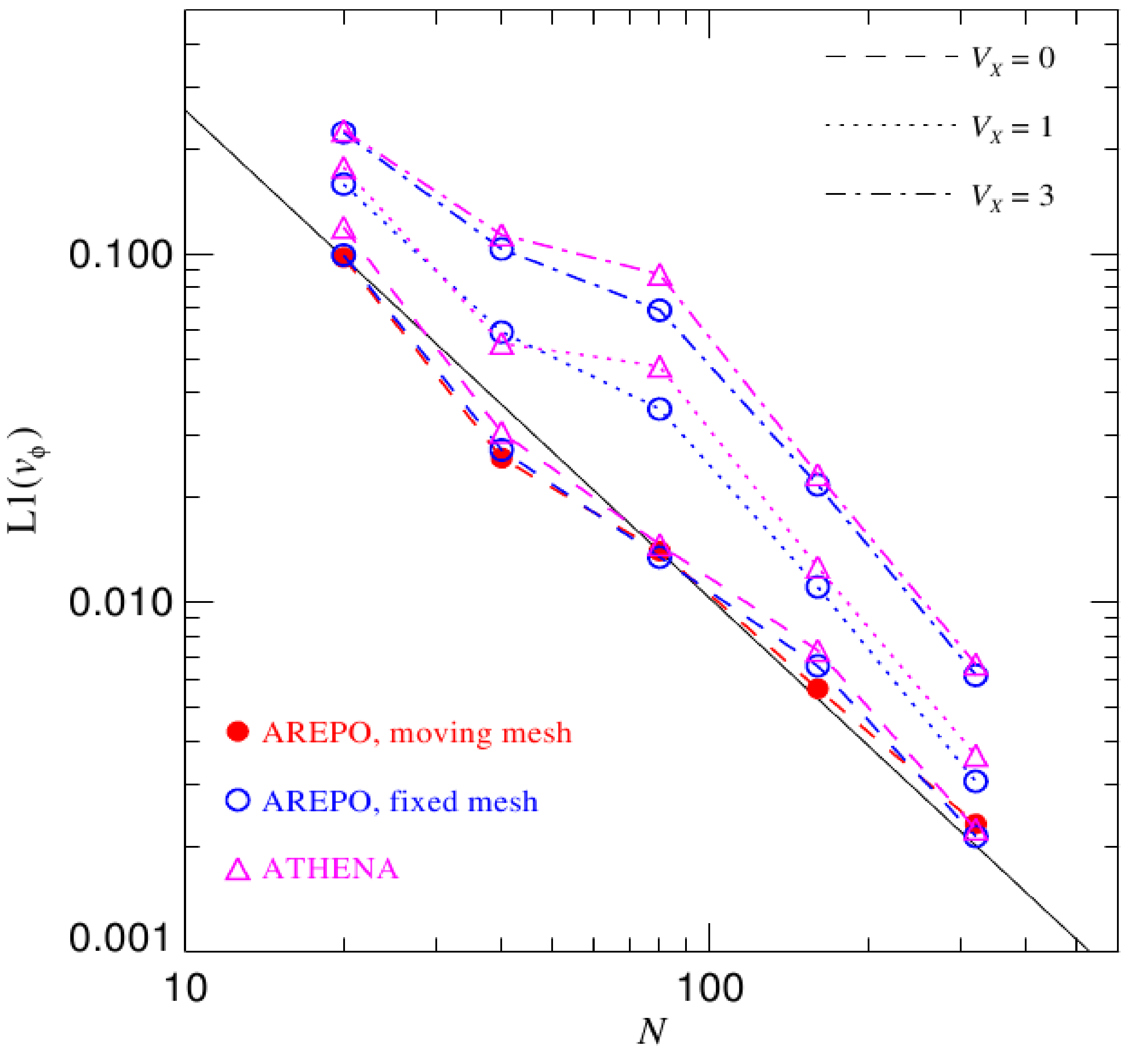

The moving-mesh approach can also be used to realize arbitrarily shaped, moving boundaries

STIRRING A COFFEE MUG

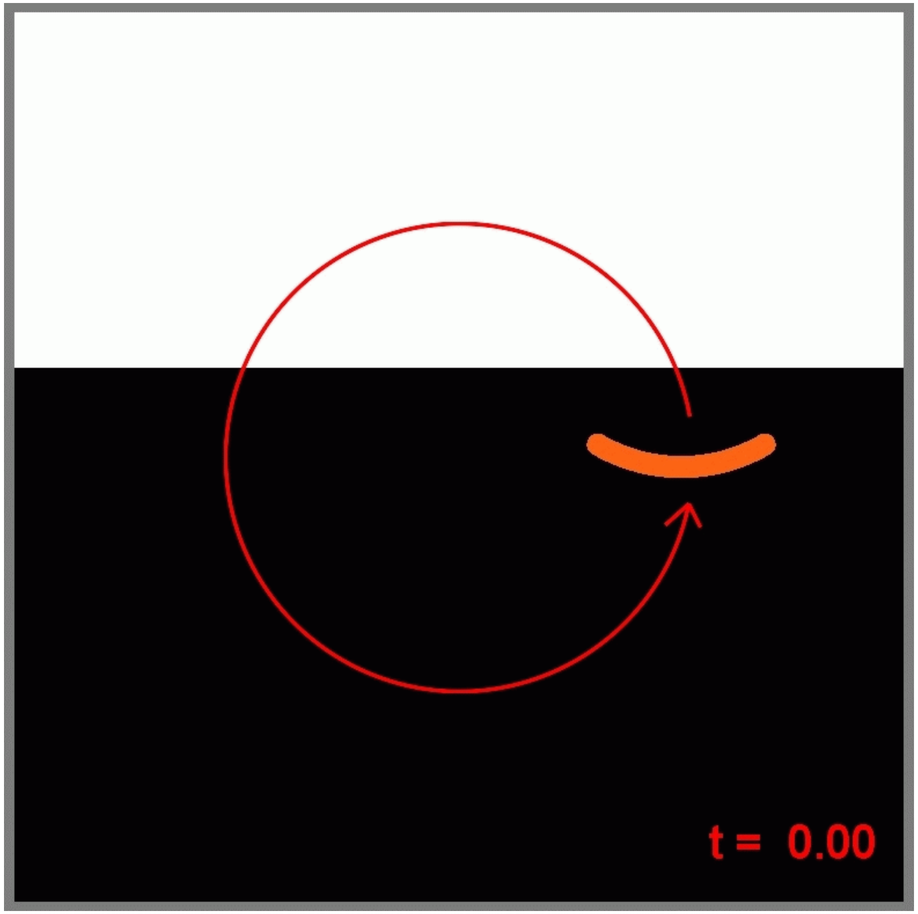

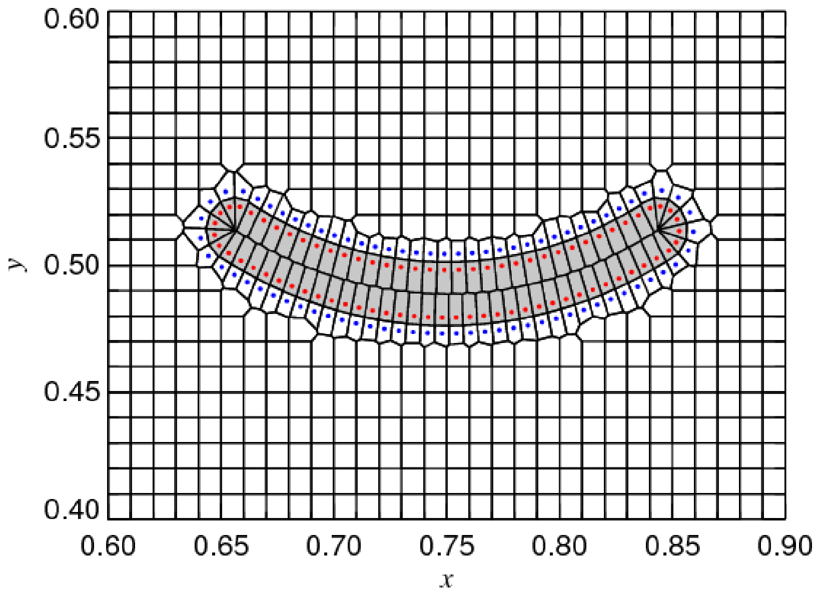

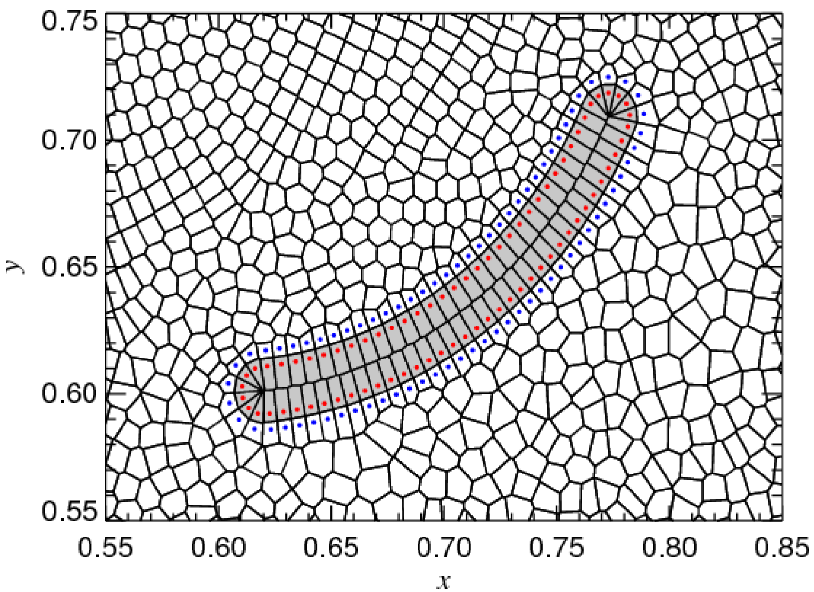

Conclusions

SPH is an incredible useful technique for astrophysics.
Its key strengths are:

- Galilean invariance (unlike Eulerian mesh codes).
- All conservation laws well fulfilled.
- Automatic Lagrangian adaptivity. Conveniently gives near ideal resolution improvements in regions that collapse.
- High geometric flexibility, vacuum boundary conditions treated easily. Code complexity limited, very robust time integration.

However, the accuracy of SPH can be a concern:

- Convergence rate for subsonic problems often poor (“noisiness” of SPH).
- Fluid instabilities poorly captured by vanilla SPH.

I expect that in the future, new improved versions of SPH, hybrid SPH/mesh or moving-mesh codes will see more use in cosmology.